NAS Technical Report; NAS-07-004
June 2007

Hemisphere Ice Ball Debris-Transport Analysis

Stuart Rogers
NASA Ames Research Center

December 2006

Contents

List of Figures

List of Tables

1 Abstract

This report documents the analysis used to determine the maximum allowable ice-ball size on the External Tank of the Space Shuttle Launch Vehicle. The maximum allowable size is determined by computing the debris transport of millions of possible ice-ball trajectories and computing over five billion possible impacts on the Orbiter, and comparing those impacts with the capability of impacted component. The impacts on the following critical components are analyzed: Orbiter wing leading-edge reinforced carbon-carbon panels, Orbiter nosecap made of reinforced carbon-carbon, and Orbiter black tiles. The primary result of the analysis is a map of the allowable ice-ball size that can be shed from the External Tank that will not exceed the impact-damage threshold for a given component. The result of this study has been incorporated as a launch commit criteria in the Space Shuttle Ice/Debris Inspection Criteria document.

2 Introduction

Under the right conditions, ice balls can form on various surfaces of the External Tank (ET) prior to launch. An example ice formation is shown in Figure 1, which is a photograph from the Space Shuttle Ice/Debris Inspection Criteria document, NSTS-08303 [1]. This ice formation is caused by chilled intertank purge gas passing through intertank stringer vent holes and exiting through a thermal protection system (TPS) defect. In the more general case, an ice ball can form anywhere on the ET once it has been filled with liquid hydrogen and liquid oxygen if there is a defect in the TPS. According to previous versions of NSTS-08303, the presence of such an ice ball on the +Z side of the ET would require engineering evaluation prior to launch. This would require an analysis of the threat of such an ice ball in less than an hour such that a go/no-go decision could be made for the launch. Under such limited time-constraints only a very simple analysis of the potential debris hazard could have been undertaken. This would likely lead to a decision to abort the launch due to the unknown debris risk. Thus there was a need for a more rigorous launch-commit criteria based upon a detailed study of the potential debris hazard posed by ice balls located anywhere on the ET. The work documented in this report is an effort to produce just such a criteria. The result of this work has now been incorporated into version D of NSTS-08303. This report specifically outlines the work leading to the maximum ice-ball data that has been labeled *Version 1.7*, and that was approved for use as a launch-commit criteria just prior to the STS-116 mission.

The current analysis uses the standard debris-transport software package, composed of the debris [2], dprox [3], and post_dprox [3] codes. This work uses release version 0.7.4 of the software, to which some additional modifications have been made. In particular, this version of the software includes the addition of a hemisphere-ice drag and cross-range model, as well as improvements to the dprox cone, and additional sorting capabilities in the dprox code. The drag and cross-range models for ice and foam that are in the debris and dprox

codes are based on unsteady, fully coupled, 6-degree-of-freedom CFD analysis of representative debris shapes [4]. The drag model in the debris code is a simple look-up table that specifies the drag coefficient as a function of the local Mach number of the local wind relative to the debris. The debris code integrates the ballistic equation of motion of the debris using a variable-step size Runge-Kutta solver, modeling the debris as a single-point mass. This process neglects any lift force that acts on the debris, however, the effect of lift is modeled in the impact detection. The dprox code performs the impact detection using a cross-range cone that is built around each individual debris zero-lift trajectory. The impact surfaces of interest, such as wing leading-edge reinforced carbon-carbon (RCC) panels, are defined as a series of discrete points and provided as input into the dprox code. Any of the impact-surface points which lie inside the cross-range cone are considered impact hits. An example of one of these cones and the zero-lift trajectory is drawn in Figure 2.

The inputs required by the debris code include CFD-generated flowfields about the Space Shuttle Launch Vehicle (SSLV) during ascent. These flowfields are interpolated to provide local gas velocity and density at each discrete point along a debris path. These CFD solutions were computed with the Overflow [8] code. The flight conditions for these ascent simulations taken from an STS-113 pre-flight day-of-launch database; these conditions include the dynamic pressure, angle of attack, side-slip angle, elevon and body-flap deflections, SSME and SRB nozzle gimble angles and their thrust levels. The CFD simulations included a simulation of the SSME and SRB plumes which used boundary conditions at the exit plane of the nozzles. The debris-transport process neglects the effect that the flying debris pieces have on the flowfield. Each of these CFD simulations include detailed representations of the Orbiter, the Solid Rocket Boosters, and the ET. This particular ET configuration is without the foam PAL ramps and with a "Reshape-1" design of the ice/frost ramps on the liquid hydrogen (LH2) portion of the tank. The CFD grid system contains 569 zones and over 76 million grid points. More information on the CFD computations of the SSLV during ascent is given in [9].

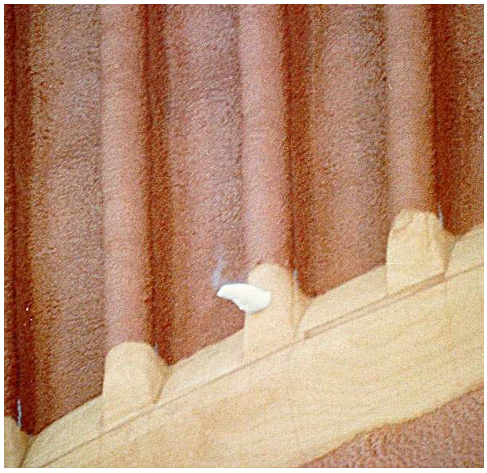

Figure 1: Photo of an ice formation on an intertank stringer.

In addition to the debris software package, a series of Perl scripts have been developed which help to automate the process running the codes over a large and varied parameter space. These scripts generate the debris input files, execute the debris and dprox codes, post-process the impact data, and generate plots

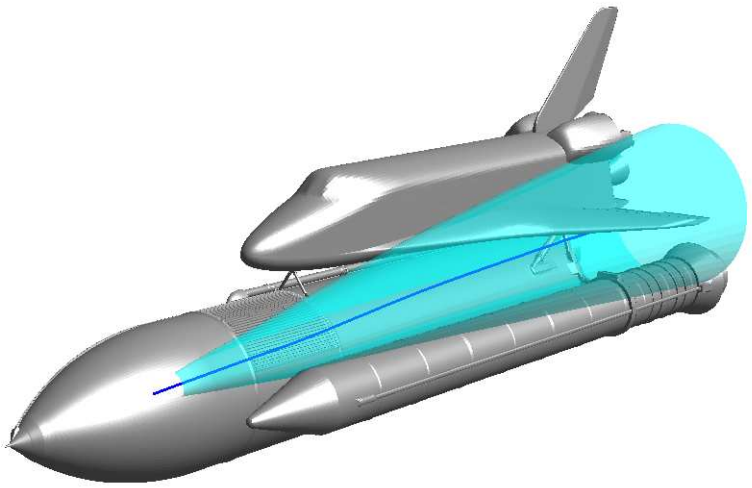

Figure 2: Example of a trajectory and cross-range cone.

of the results. All of the computed results reported in the current work were generated on the NASA Ames supercomputer system known as Columbia. This system is composed of a total of over 10,000 Intel Itanium2 processors. All CPU times reported herein are computational times on these processors.

The remainder of this this report is organized as follows. A section that gives a detailed description of the inputs and assumptions for the current analysis is provided. The next section presents the models which were used to represent the ability of the RCC and tiles to withstand the ice-ball impacts. Following that is a description of the computational procedure used in this work. The final section contains a summary of the computed results, including a number of sample debris trajectories and the resulting impact conditions and computed damage. The appendices include tables describing the ice-ball masses and sizes used in the analysis, a table listing the flight conditions in the CFD flow-fields used in the debris transport analysis, and finally, tables listing the final result of this work: the maximum allowable ice-ball diameter as a function of XT and ϕ location on the ET.

3 Inputs and Assumptions

Ice formations in this analysis are modeled as hemispheres, as this is a general shape which is representative of a number of actual ice formations seen on past flights. Given an input mass and the ice density, the hemisphere diameter can

be computed, and this is enough information to create the debris-code inputs required to describe the piece of ice debris. The nominal hemisphere drag model in the debris code was used to model the aerodynamic drag of the ice balls. A detailed study of the composition of ice balls that can form on the ET was undertaken by Project Iceball [5]. This study found that two distinct iceball morphologies are possible, dependent on the environmental temperature and humidity. One morphology is shaped as a hemisphere with a thick shell of ice and is possibly filled with frost. This thick-shelled ice-ball morphology is illustrated in Figure 3. The results of Project Iceball showed that a typical thick-shelled ice ball has only a small core of frost whose diameter is approximately 20% of outer diameter, or $OD = 0.2ID$. The other type of ice ball is composed of a ring of solid ice, a thin outer shell of solid ice, and frost in the center. This thin-shelled ice-ball morphology is illustrated in Figure 4. In both morphologies, the frost is fluffy and does not hold together when subjected to any significant aerodynamic force, and thus the mass of the frost is not included in the debris analysis.

The current analysis models each of these two morphologies as solid hemispheres with a uniform density. The thick-shelled ice ball was modeled with an ice density of 47 lbm per cubic foot (pcf), and the thin-shell ice ball used an ice density of 27 pcf. These ice densities are based on the measurements of the ice size and mass from Project Iceball. Note that from an aerodynamic point of view, for a given mass, the 27 pcf density case will usually result in a greater threat. This is because for a constant mass, the 27 pcf hemisphere would be larger, have a smaller ballistic number, and thus provide less resistance to the airflow and create greater impact velocities than the 47 pcf case.

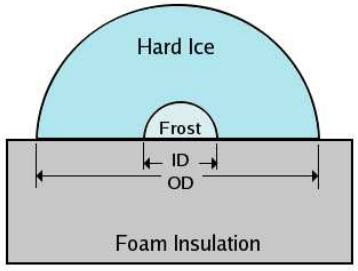

Figure 3: Thick-shelled ice-ball geometry.

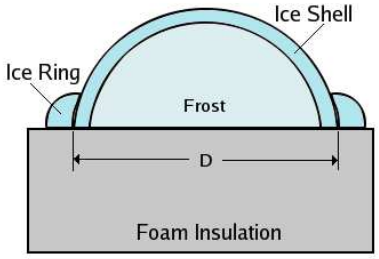

Figure 4: Thin-shelled ice-ball geometry.

The table of ice-ball sizes used as a launch-commit criteria will contain the observed ice-ball diameter; the debris transport masses will be that of the liberated ice ball. In order to build a table of the maximum allowable ice-ball size, a model of the relationship of the liberated mass to the observed size is required. Following the recommendation of the ET project, it is assumed that two-thirds of the mass of the thick-shelled ice balls will liberate. The relationship between the liberated mass m_{thick} and the

observed outer diameter of the thick-shelled ice balls is given by:

$$m_{thick} = \frac{2}{3}\rho_{ice}\frac{\pi}{12}[OD^3 - ID^3]$$

where OD is the observed outer diameter of the ice ball, and ID is the diameter of the frost core. Using $ID = 0.2OD$, and $\rho_{ice} = 47$ pcf, the liberated mass is:

$$m_{thick} = 0.004709\ OD^3$$

where OD is in inches and m_{thick} is in lbm.

For thin-shelled ice balls it is assumed that the liberation mass will be that of an ice hemisphere of 27 pcf density whose outer diameter matches the inner diameter D of the ice-ring, as illustrated in Figure 4. Thus the liberated mass m_{thin} of the thin-shelled ice ball is given by:

$$m_{thin} = \rho_{ice}\frac{\pi}{12}D^3$$

Using $\rho_{ice} = 27$ pcf, the liberated mass is:

$$m_{thin} = 0.004091\ D^3$$

where D is in inches and m_{thin} is in lbm.

A comprehensive list of 35 possible different ice-ball masses were analyzed in the current work ranging from 0.0002 to 0.05 lbm. The actual mass values are listed in Table 1 in the appendix. This table also lists the corresponding hemisphere diameter for the liberation mass, as well as the corresponding observable diameter of the ice ball before liberation. These quantities are also illustrated in a plot of diameter versus mass versus in the appendix.

The exact physical mechanism by which the ice balls might be released into the flowfield is not known, but there is no reason to believe that the ice would have an appreciable initial pop-off velocity. It was noted that during some initial test runs, many of the ice debris pieces would never leave the boundary layer if released with zero initial velocity. In this case the debris trajectories would stop right away as they struck the ET wall. For this reason, all debris pieces were released with initial velocities of zero and 5 feet per sec, normal to the surface.

It is not known where ice balls will form on the ET, nor when ice debris may be released during the ascent, and thus this analysis must search through all possible release locations and flight Mach numbers to find the worst possible impacts. The ice balls release locations used in the current work are plotted as blue dots on the surface of the ET in Figure 5 and Figure 6. These locations extend from ET coordinates of XT=371 inches to XT=2100 inches, and circumferentially from ϕ=-110 degrees to ϕ=110 degrees. The release locations are spaced 12 inches apart in XT and 4 degrees in ϕ. The ice balls are released one inch above the surface of the ET. No ice balls were released from the "no-ice zone". This is a region on the forward portion of the ET where ice is not allowed and would result in a violation of the existing launch commit criteria.

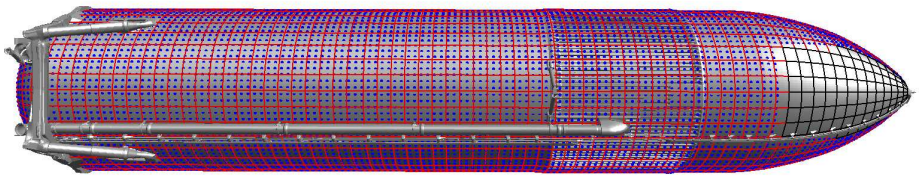

Figure 5: Release locations of ice debris.

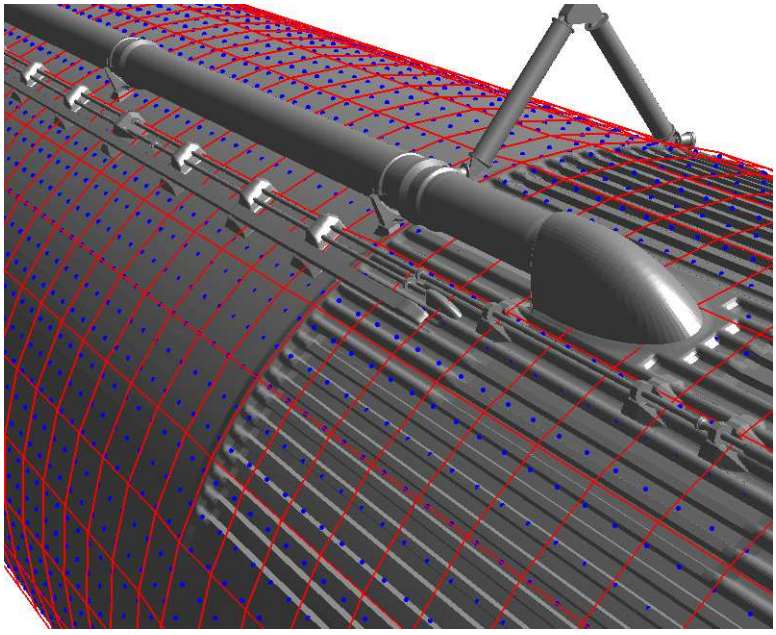

Figure 6: Close-up view of release locations near the intertank region of the ET.

The ice-ball debris-transport analysis was computed using a large number of flight conditions representing both nominal ascent conditions as well as design-dynamic pressure conditions with dispersions in the vehicle angle of attack and side-slip angle. The flow-fields representing the nominal flight conditions utilize an STS-113 day-of-launch pre-flight nominal trajectory database to set angle of attack, side-slip angle, dynamic pressure, thrust settings, gimble angles, and control-surface deflections. These cases were run for Mach number of 0.6, 0.9, 1.05, 1.1, 1.25, 1.4, 1.55, 1.8, 2.0, 2.2, 2.5, 2.75, 3.0, and 3.5. An additional 17 different CFD solutions at design dynamic pressure conditions for Mach numbers of 1.4, 1.55, 1.8, and 2.2 were used in the analysis. These latter CFD flow-fields were run with angles of attack and side-slip angles dispersed from the nominal flight trajectories. A plot of the CFD angle of attack and side-slip angles used here is plotted along with the historical flight envelope as a function of Mach number in Figure 7 and Figure 8. Table 2 in the appendix lists the conditions of all 31 of CFD cases used in this analysis.

A summary of the inputs are listed here:

- 7635 release locations: $371in \leq XT \leq 2100in$, -110 deg $\leq \phi \leq$ 110 deg
- 14 Mach numbers at nominal dynamic pressure : 0.6 to 3.5
- 17 Mach numbers at design dynamic pressure : 1.4 to 2.2
- 2 initial pop-off velocities: 0.0 and 5.0 ft/sec
- 35 masses: 0.0002 lbm to 0.05 lbm
- 2 ice densities = 27 and 47 pcf
- Over 33 million debris trajectories total

The dprox code inputs are described here. The cone algorithm uses the 3σ cross-range model for hemispheres that is in the dprox code. Three other changes to the default dprox code inputs were made for the tile impacts only. The cone-extrapolation feature was turned off for the tile calculations as it was found that this was causing the code to predict many non-physically possible, high-angle impacts for ice-ball trajectories which terminate when they hit the aft-attach hardware. Also, the cone-segment length was reduced from 50 inches to 5 inches in order to increase the fidelity and resolution when constructing the cones. The dprox code has a blanking feature which eliminates hits that cannot occur because the impact surface is downstream of an obstructing surface. The blanking feature can be used to eliminate physically impossible impacts that are otherwise predicted by the cone algorithm. This feature was used when computing the tile impacts in the current work. The input blanking surfaces that were provided to the software include the bipod struts, the liquid oxygen (LO2) feedline, and the aft attach hardware on the ET; these are illustrated in Figure 9.

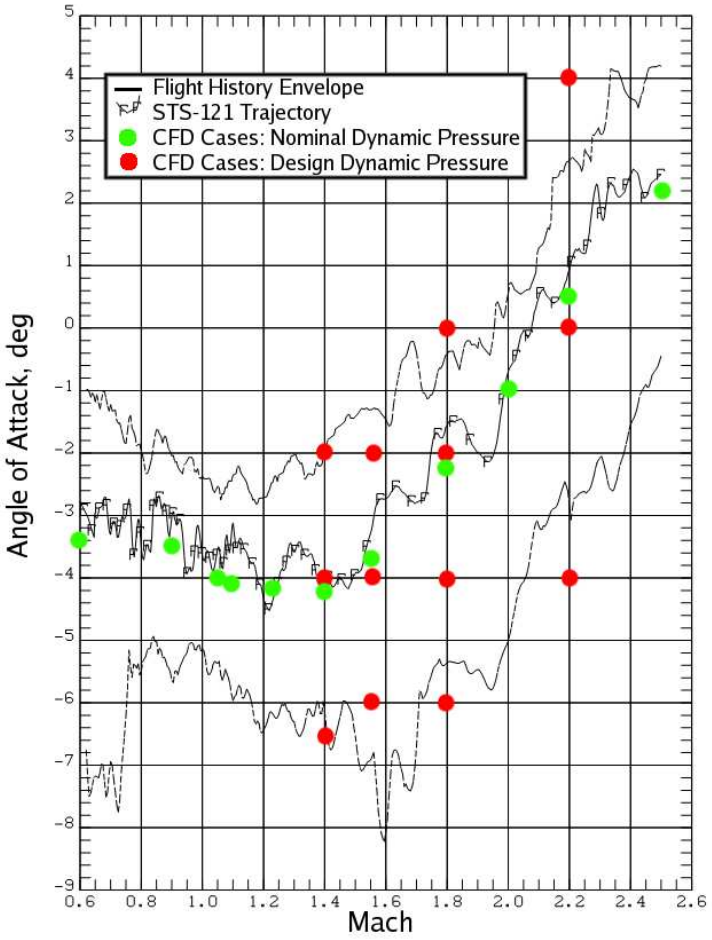

Figure 7: Angle of attack versus Mach number.

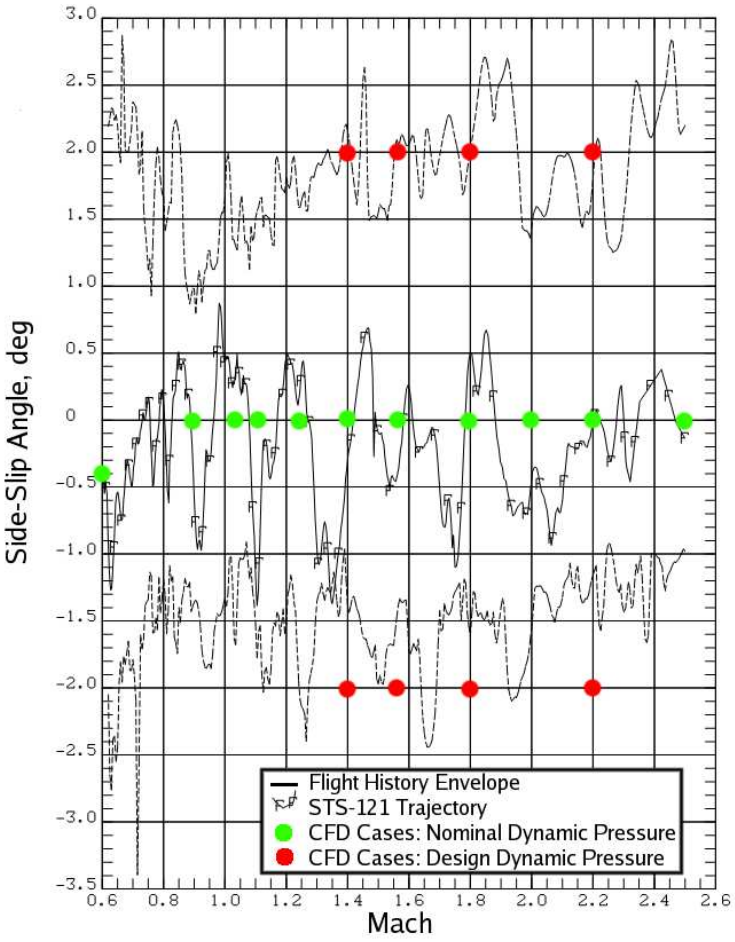

Figure 8: Side-slip angle versus Mach number.

The following is a list of additional assumptions used in this analysis. The ice debris is assumed to be homogeneous, and the debris is modeled as a smooth hemisphere with no account for roughness. The debris is assumed to remain whole in flight and does not break up. When the debris strikes a surface the simulation of that debris stops, no rebounds are simulated. While the debris code can simulate rebounds, the coefficient of restitution for ice impacts is currently unknown, and it is thought that it is probable that a collision would cause the ice to break up.

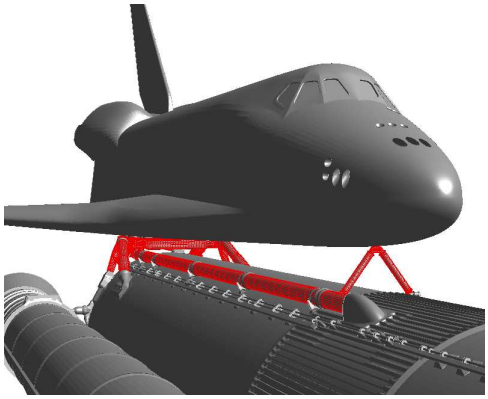

Figure 9: Surfaces used for the blanking feature in dprox.

4 Capability and Damage Models

Each impact that is computed by the dprox code is evaluated to determine if it is acceptable or unacceptable. This section describes the models and criteria which are used to make this acceptability evaluation. The evaluation computes a C/E ratio, where C represents the capability of the impacted surface to withstand the impact, and E represents the environment as represented by the particular debris impact. The impacts on the RCC components are quantified by the kinetic energy of the impact, and the impacts on the Orbiter tiles are quantified by the depth of the damage, if any, that the impact creates.

4.1 RCC Capability

The ice-on-RCC impact capability numbers used in the current work are the certification-rigor kinetic-energy capability values provided by the Orbiter project [6]. The capability for the RCC nosecap is 16 foot-pounds (ft-lbs). There are separate capability values for each of the wing-leading-edge RCC panels. The panels are numbered 1-22 going inboard to outboard on both the port and starboard wings. The capability kinetic energy for panels one through four is 136 ft-lbs, for panels five through seven is 53 ft-lbs; for panels eight through 12 is 48 ft-lbs, for panels 13 through 15 is 53 ft-lbs, for panels 16 through 18 is 58 ft-lbs, and for panels 19 through 22 is 136 ft-lbs.

These wing leading-edge capability values are adjusted for each impact by two different factors. The first is a mass-adjustment factor which reduces the capability for masses which are smaller than 0.02 lbm and increases the capability

for masses which are larger than 0.02 lbm. This factor is given by:

$$f_{mass} = \left[\frac{m}{0.02}\right]^{0.3}$$

where m is the mass of the ice-debris impactor in lbm. The second is an impact-angle factor which will increase the capability for impacts of with shallower angles, but is applicable only to wing-leading edge panels nine through 19. This factor is given by:

$$f_{angle} = \frac{1}{2[sin(\frac{\pi}{4} - \beta_{impact})]^2}$$

$$\beta_{impact} = tan^{-1}\left(\frac{V_y}{V_x}\right) \text{ for starboard} - \text{wing impacts}$$

$$\beta_{impact} = tan^{-1}\left(\frac{-V_y}{V_x}\right) \text{ for port} - \text{wing impacts}$$

where V_x and V_y are the x-component and y-component of the impact velocity vector, respectively. Also, β_{impact} is limited to eight degrees, and thus $f_{angle} \leq 1.38$.

4.2 Tile Damage Model

The tile damage model is used to predict the depth of damage that will occur as a function of the impact velocity magnitude and the impact angle. The model used in the current work is known as the Southwest Research Institute 95% bounding ice-on-tile damage model [12]. The tile-damage model has certain limits on its range of applicability which are listed here. The impact angle must be greater than or equal to 5 degrees; the software enforces this restriction by rounding all smaller impact angles up to 5 degrees. The code also enforces the restriction that for any impact angle that is greater than 20 degrees, the ice density should be rounded up to 57 pcf. Other restrictions to this model that be less than 1.0 lbm; the ice density range should be between 31 and 57 pcf; the impact velocity magnitude should be less than 1500 feet/sec; and the aspect ratio should be greater than 2.5 for any impact angles that are greater than 60 degrees.

4.3 Tile Capability

The allowable tile damage depth used in this analysis is the mean/expected tile-damage-depth capability, see [10] and [11]. This lists an allowable damage-depth capability for the tiles, grouped by zones on the bottom surface of the orbiter. The mean/expected tile-damage depth capability is plotted in Figure 10. The color represents the maximum allowable tile damage depth in inches. The borders of the tile zones are outlined in black.

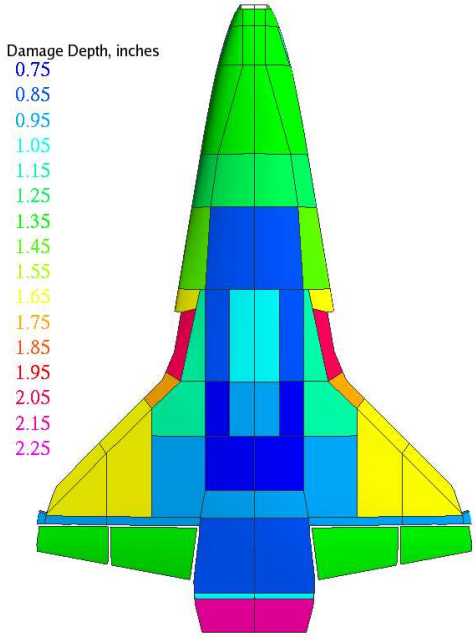

Figure 10: Mean/expected allowable damage depth for Orbiter tiles.

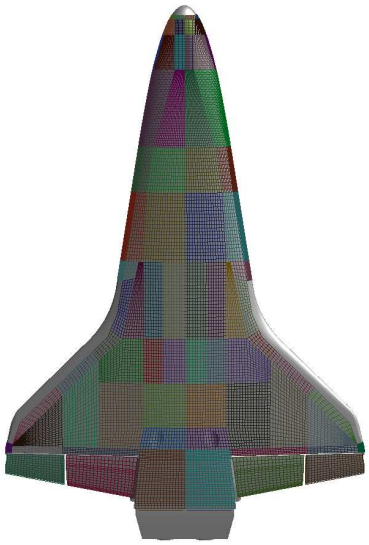

Figure 11: Impact grids on the Orbiter under-side tiles.

4.4 Impact Surfaces

The impact surfaces which are used by the dprox code to detect ice-ball impacts on the Orbiter under-side tiles are illustrated in Figure 11. The tile impact grid contains 74 zones and 17,660 grid points. The grid spacing on the tiles is 6 to 8 inches on the flat tile regions, and is 2 to 3 inches in regions of greater curvature.

The impact surfaces which are used by the dprox code to detect ice-ball impacts on the Orbiter RCC panels are illustrated in Figure 12 and Figure 13. The nosecap RCC impact grid contains a single zone with over 1100 grid points. The wing RCC impact grid contains 44 zones, one zone per RCC panel, and a total of 33,200 grid points. The grid-spacing in the both the wing and nosecap RCC is between 1.0 to 2.0 inches, which provides more than adequate resolution of the impacts on these surfaces.

5 Procedure

The procedure for computing the maximum allowable ice-ball size on the ET surface for a given impact target is detailed here. The calculations are launched and processed within a series of Perl scripts. Several standard Shuttle-debris scripts exist which have been developed by the author and have been used for many different debris cases. These standard scripts are used to generate the debris-code input files, and to execute the debris code. A single debris-code input file is generated for each combination of Mach number, mass, and ice density; each of these single executions of the debris code generates on the

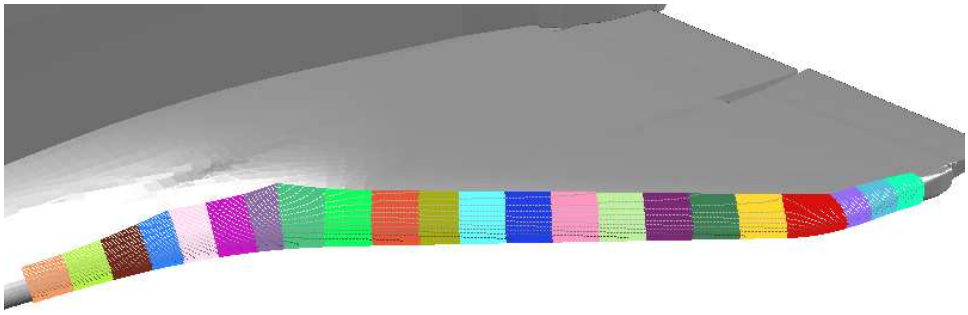

Figure 12: Impact grids on the left-wing RCC panels.

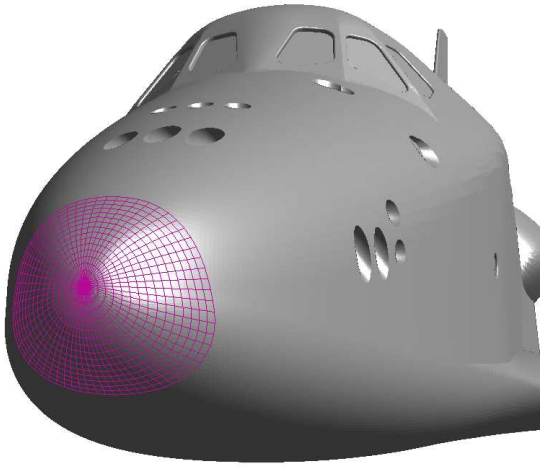

Figure 13: Impact grid on nosecap RCC panel.

order of 15,000 debris trajectories. The debris code requires on the an average of 0.3 CPU seconds per trajectory, and over 33 million debris trajectories were computed, for a total of approximately 2750 CPU hours.

In running the dprox code and computing the impacts for all of these trajectories, we need to map the C/E ratio resulting from each impact back to each source location, and do this individually for each mass, and for each ice density. Because of the sheer number of debris trajectories that are involved some special procedures had to be developed to compute the impact data. The dprox code could not be run for all 10,000 trajectories from a single debris-code run at once: without any filtering of the hits, this would result in an output file containing 500 million hits and 10 gigabytes in size, and this would have to be repeated thousands of times. Running this for all cases results in terabytes of storage requirements. If dprox is run with filtering to keep just the lowest C/E impact at each impact point, this would throw away too much information, as we need to know the worst hit as a function of release location. Finally, we cannot go back and execute the debris code for each individual release location due to the high overhead cost of starting the code because it has to read in the entire CFD grid and solution for the SSLV.

The solution to this problem was to add a new filter option to the dprox code that selects specific trajectories from the debris output file to be analyzed in the current run. This included the ability to select the trajectories as a function of the debris release locations. Then in order to control the number of dprox executions, the ET surface was broken up in to subsets, each of which contain several release points. Each such ET-surface subset is 25 inches along the axial direction and 10 degrees circumferentially, as illustrated by the red grid in Figure 5 and Figure 6. There are 990 ET-surface subsets. The procedure then executes dprox for each ET-surface subset, using the new filter to select only those trajectories which start in the current subset, and it filters the impact data to keep the minimum C/E hit at each target point. Thus at the end of each dprox run, the process extracts the worst impact conditions for the given ET-surface subset, and then deletes the dprox output file. At the end of the dprox runs the procedure has stored the worst impact conditions for each ET-surface subset for each mass, each Mach number, and each ice density. A perl script was written to execute this procedure automatically.

6 Ice-ball Results

The final results from this analysis are presented here. Colored symbols illustrating the maximum allowable ice-ball diameter, in inches, on the surface of the ET are shown in Figures 14 and 15 for thin-shelled ice balls and thick-shelled ice balls, respectively. Three views of the ET are shown in each of these figures, one showing the -Y side of the tank, one showing the +Z side, and a third view showing the +Y side. In these two figures, the no-ice zone [1] on the surface of the ET is covered with black symbols. The data that is represented in these plots is also listed in tables in the appendix at the end of this report.

The diameters presented here are the diameters of the observed ice balls as they exist on the tank before launch. For the thin-shelled ice balls, the quantity that is plotted is that of the inner diameter D of the ice-ball ring as illustrated in Figure 4. For thick-shelled ice balls, the quantity plotted here is the outer diameter OD as illustrated in Figure 3. The magenta-color symbols indicate that the maximum-sized ice ball that was used in this analysis (corresponding to 0.05 lbm release mass) is allowed from that location. In nearly all instances this result was obtained because there was no debris transport mechanism from this location to any of the impact surfaces.

A comparison between the results from impacts on each of the three different impact surfaces is shown in Figures 16 and 17 for thin- and thick-shelled ice balls, respectively. Each of these two figures show separate results for the impacts on the tiles, wing RCC, and nosecap RCC. These figures show that the limitations on the LO2 and intertank regions of the ET are driven primarily by impacts to wing RCC panels. The impacts to the tile dominate the final ice-ball allowables aft of XT=1400 inches. One can also see that while it is possible to get nosecap impacts from the forward portion of the ET, none of these impacts result in limitations to the final maximum allowable ice balls.

6.1 Ice-Ball Trajectories

In this section some specific ice-ball trajectories are examined in an effort to understand the results in greater detail. First, some ice-ball trajectories from some historically observed ice-ball locations are presented. Following these are some example trajectories taken from some of the zones which show restrictive or surprising results.

6.1.1 ET/SRB cable-tray acreage

While there is no definitive record of all of the ice balls that have formed on the ET during previous launch attempts, one location that has formed ice balls in the past is the aft-end of the ET near the ET/SRB cable-tray acreage interface, located between XT = 2064 to 2067 inches and between ϕ = 45 to 54 degrees. Photographs of two such ice balls are shown in NSTS08303 in Figures 3.3.5c and 3.3.5d. This location is circled in a close-up of the maximum allowable ice-ball plot in Figure 18. Some example trajectories of ice balls released from this location are shown in Figure 19. The debris in these trajectories are mass = 0.05 lbm thick-shelled ice balls released into the Mach = 1.5, α = -4 deg, β = -2 deg flow-field. This specific set of trajectories caused the worst tile damage out of all of the cases where were analyzed. They result in many possible impacts on the orbiter tiles, but none of the impacts result in a damage depth greater than that allowed for these tile zones. The impact velocity magnitude and the impact angle, as well as the maximum damage depth are plotted in Figure 20. The impact velocities of these impacts are very low, and although the impact angles are relatively large, the maximum damage depth is less than an inch.

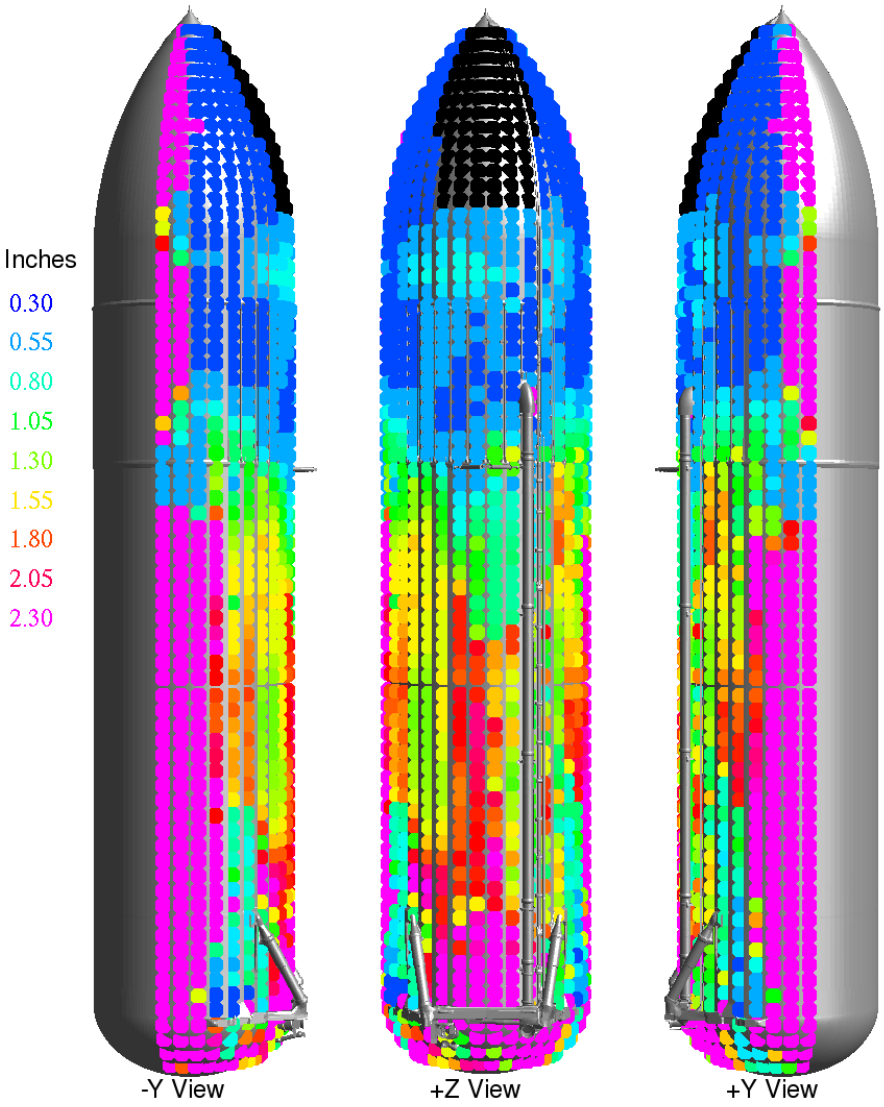

Figure 14: Maximum allowable diameter for thin-shelled ice balls.

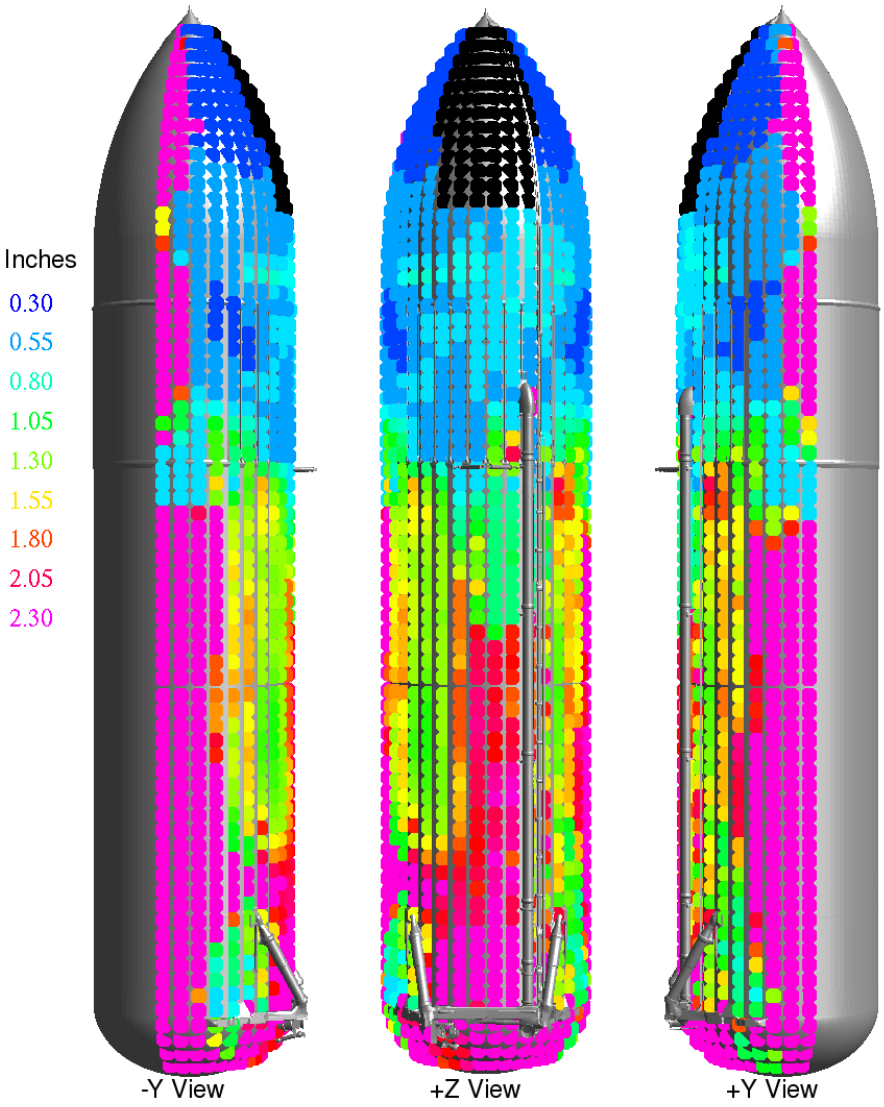

Figure 15: Maximum allowable diameter for thick-shelled ice balls.

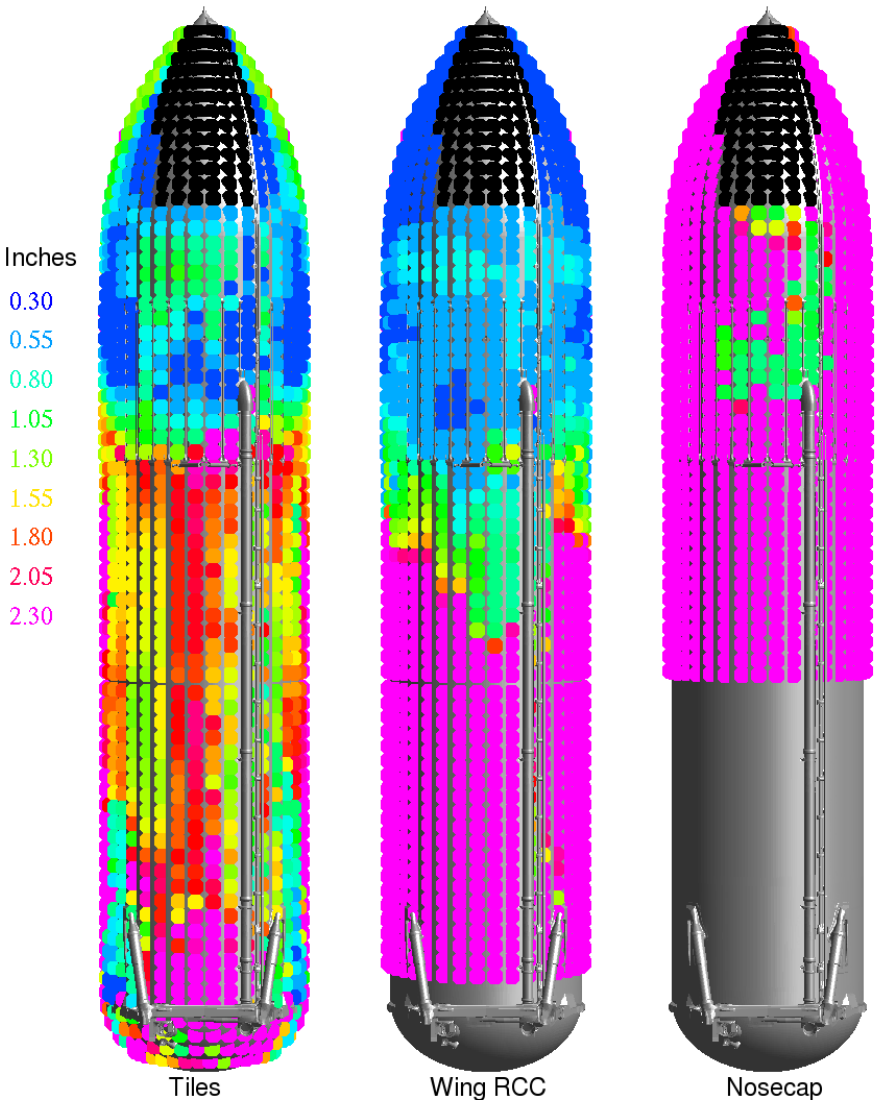

Figure 16: Comparison between tile, wing RCC, and nosecap RCC allowable thin-shelled ice balls.

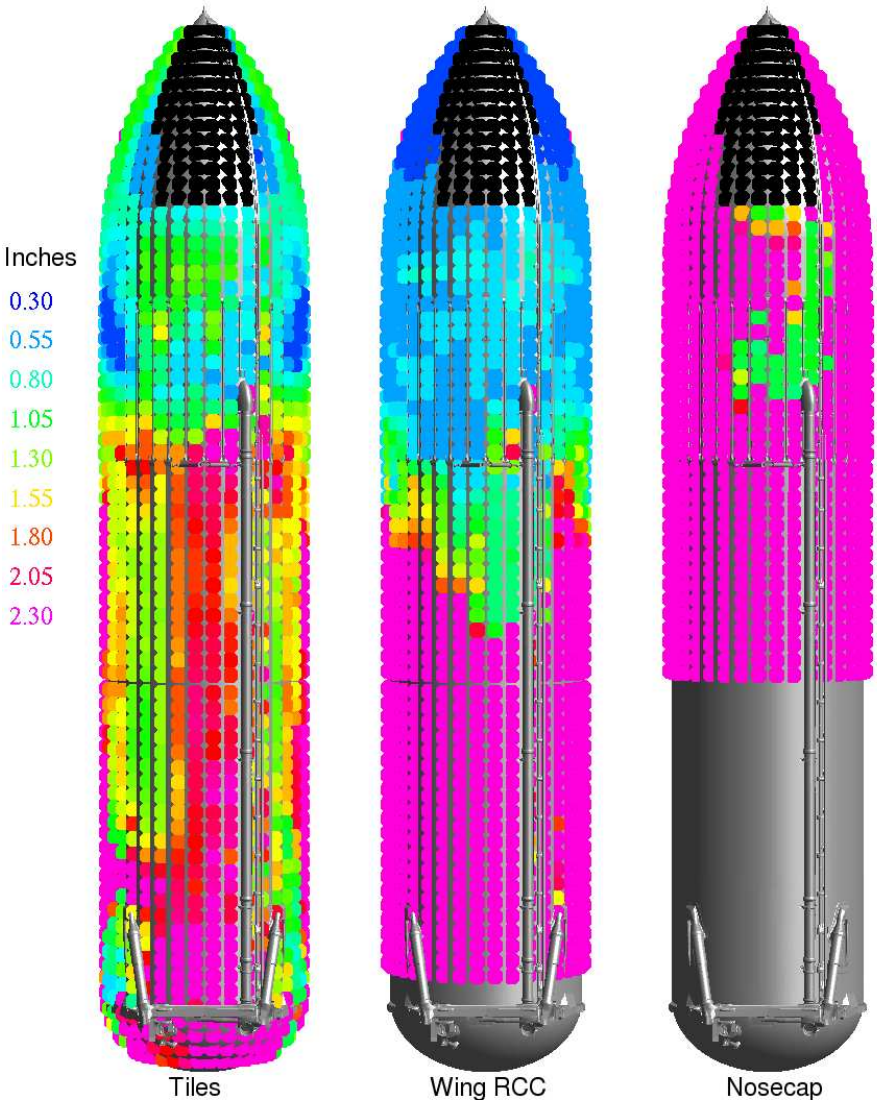

Figure 17: Comparison between tile, wing RCC, and nosecap RCC allowable thick-shelled ice balls.

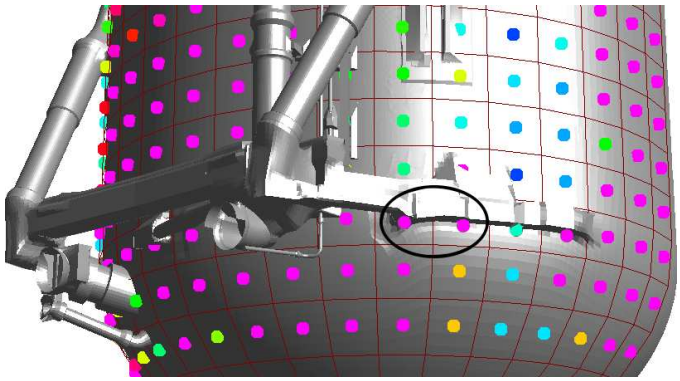

Figure 18: Maximum ice-ball diameters in the vicinity of the ET/SRB cable-tray acreage interface.

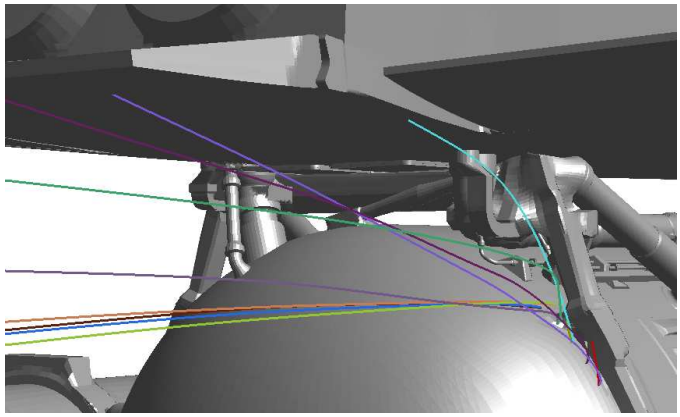

Figure 19: Trajectories of ice balls released near the ET/SRB cable-tray acreage interface.

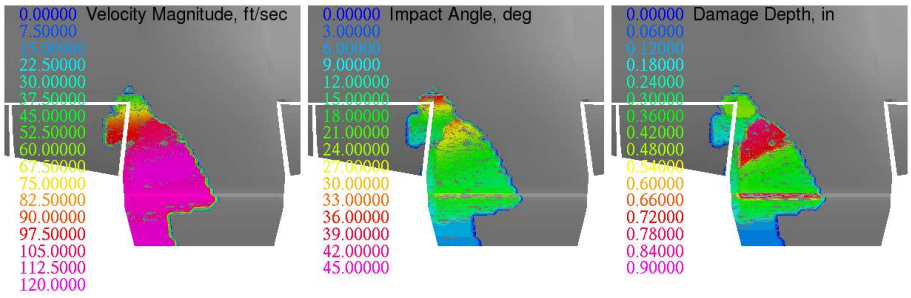

Figure 20: Impact conditions and tile-damage depth caused by the ET/SRB cable-tray ice balls, mass=0.05 lbm, Mach=1.5, α=-4 deg, β=-2 deg.

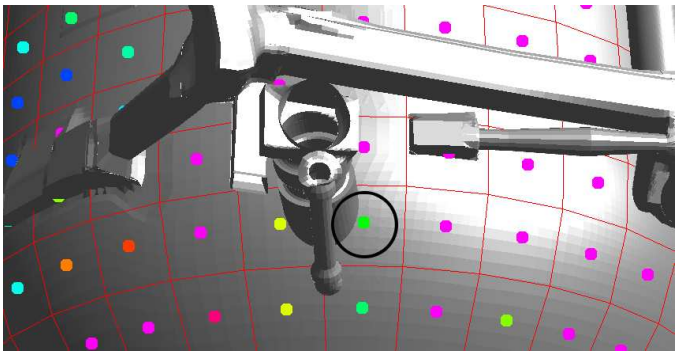

Figure 21: Maximum ice-ball diameters in the vicinity of the LH2 Umbilical.

6.1.2 LH2 Umbilical

During one of the STS-114 pre-flight tankings an ice ball formed at the base of the LH2 umbilical. This location is within the quadrant bounded by XT = 2075 to 2100 inches and ϕ = -20 to -10 degrees. A close up view of this location of the ice ball allowable size contour plot is shown in Figure 21. The maximum allowable diameter for thin-shelled ice balls in this quadrant is 1.07 inches. The worst damage from an allowable ice ball was computed from a release at Mach=1.8, α=0, β=0. Example ice-ball trajectories released from this location at these conditions are shown in Figure 22 for an ice ball mass of 0.006 lbm. The impact velocity magnitude, impact angle, and the maximum damage depth for these trajectories are plotted in Figure 23. The worst damage resulted from the direct, high-angle impact of the blue trajectory. Ice balls of masses larger than 0.006 will cause similar impacts with deeper damage that exceed the allowable damage depth.

6.1.3 Outboard of Longeron

Another region of interest is the very small allowable ice-ball sizes in the region outboard of the starboard longeron in the zone from XT=1950 to 1975 inches and ϕ=60 to 70 degrees. The maximum thin-shelled ice ball size for this region is 0.53 inches, as plotted in Figure 24. The worst damage from an allowable ice ball from this zone was computed from a release at Mach=1.8, α=-2, β=2. Example ice-ball trajectories released from this location at these conditions are shown in Figure 25 for an ice ball mass of 0.0006 lbm. These trajectories tend to fly up and inboard directly toward the orbiter tiles. The impact velocity magnitude, impact angle, and the maximum damage depth for these trajectories are plotted in Figure 26. These trajectories result in fairly high-speed impacts on the order of 500 feet per second and substantially high angles, and thus even very small masses can create substantial damage.

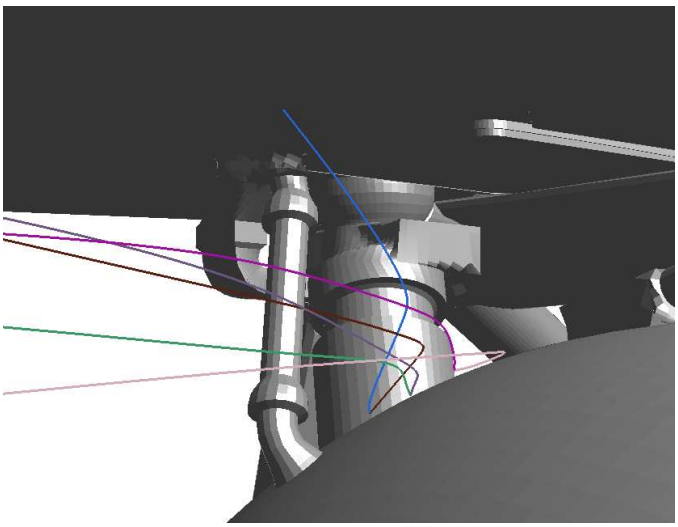

Figure 22: Trajectories of ice balls released near the LH2 Umbilical.

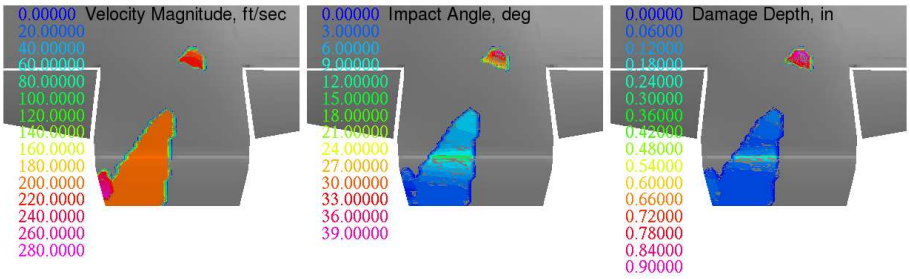

Figure 23: Impact conditions and tile-damage depth caused by the LH2 Umbilical ice balls, mass=0.006 lbm, Mach=1.8, α=0 deg, β=0 deg.

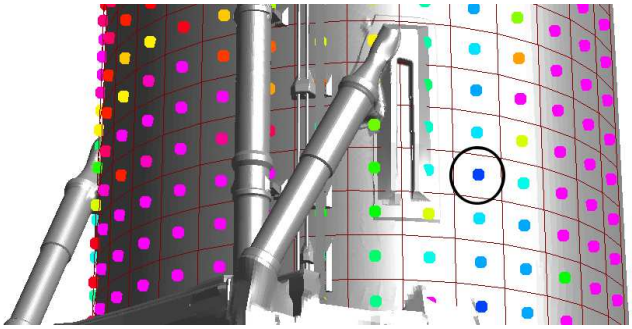

Figure 24: Maximum ice-ball diameters outboard of the starboard longeron.

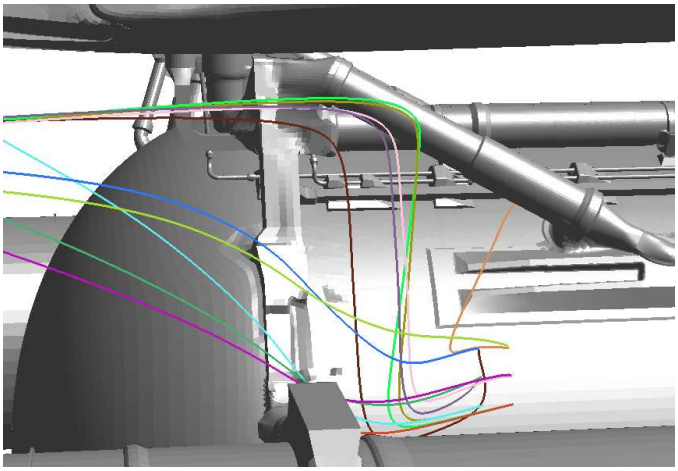

Figure 25: Trajectories of ice balls released outboard of the starboard longeron.

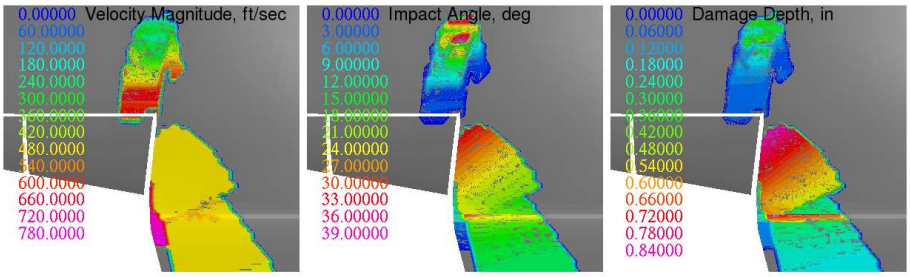

Figure 26: Impact conditions and tile-damage depth caused by the ice balls outboard of the starboard longeron, mass=0.0006 lbm, Mach=1.8, α=-2 deg, β=2 deg.

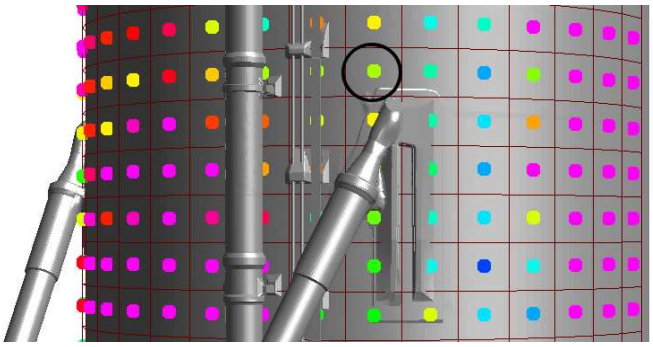

Figure 27: Maximum ice-ball diameters upstream of the starboard longeron.

6.1.4 Upstream of Starboard Longeron

Another region of interest is just upstream of the starboard longeron, where the wing-RCC-only results in Figure 16 and Figure 17 show that RCC impacts are possible from a relatively aft release location. The aft-most RCC impacts come from the region from XT=1850 to 1875 and ϕ=40 to 50 degrees. The maximum thin-shelled ice ball diameter allowable in this region is plotted in Figure 27. The maximum diameter in the circled zone in this figure is 1.43 inches. The impacts that cause this limitation occur only for the flight conditions of Mach=1.4, α=-4 degrees, β=-2 degrees. One trajectory of interest released from this zone at these conditions is shown in Figure 28. This trajectory travels a significant distance upstream due to some reverse flow, and then travels upward and back downstream. Also shown in this figure is the cross-range cone which is used to determine all possible impacts from this trajectory. It can be seen that the outer edge of the cone intersects part of the leading edge RCC panels on the starboard wing. These impacts on the wing RCC are driving the limitations on the ice balls from this zone. The fact that these RCC impacts occur only at this flight condition and that the impacts occur only on the outer edges of the cone mean that there is only a very low probability of impacts occurring.

6.1.5 Aft-Most Releases

The aft-most ice-ball zones that were studied extend from XT=2125 to 2150 inches. One of the more restrictive thin-shelled allowable diameters in this aft-most row is 0.76 inches for ϕ=70 to 80 degrees. A plot of this region is shown in Figure 29. Ice balls released from this zone impact the tiles only under a few of the flow conditions. One such example is shown in Figure 30 which illustrates the ice-ball trajectories for a mass of 0.0022 lbm released in a Mach=1.4 flow-field at α = -4, β=-2. This figure also shows the dprox cross-range cone which results in the worst impact conditions. It can be seen that the outer edge of this cone intersects only one corner of the body flap, and that the probability of such an impact occurring is relatively low. The impact velocity magnitude,

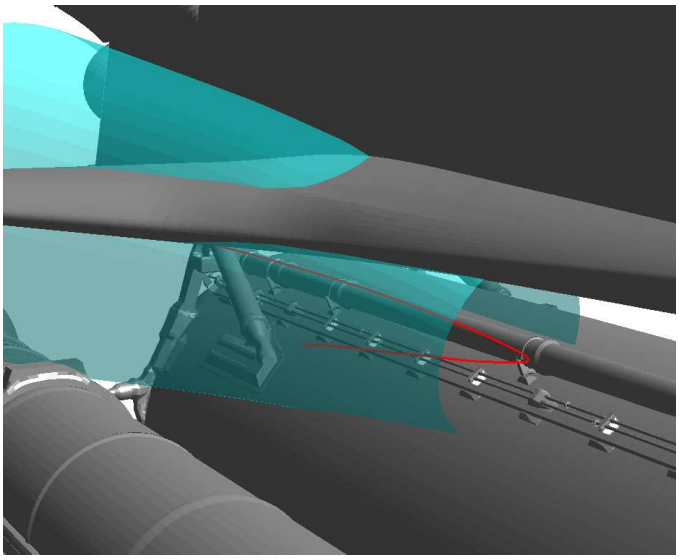

Figure 28: Trajectories of ice balls released upstream of the starboard longeron.

impact angle, and the maximum damage depth for these trajectories are plotted in Figure 31. It can be seen that the critical damage created by these impacts is confined to a very small region upstream of the body flap. The body flap itself can withstand damage depths over two inches, while the tile zone just in front of the body flap is limited to about one inch, as can be seen in Figure 10.

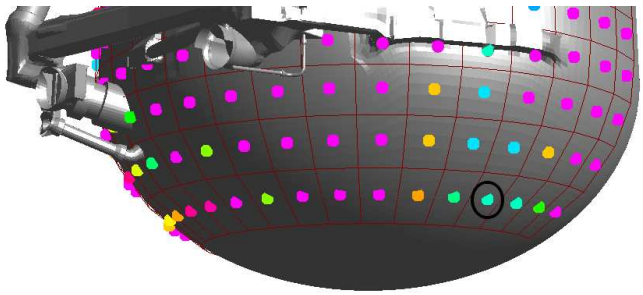

Figure 29: Maximum ice-ball diameters in aft-most region.

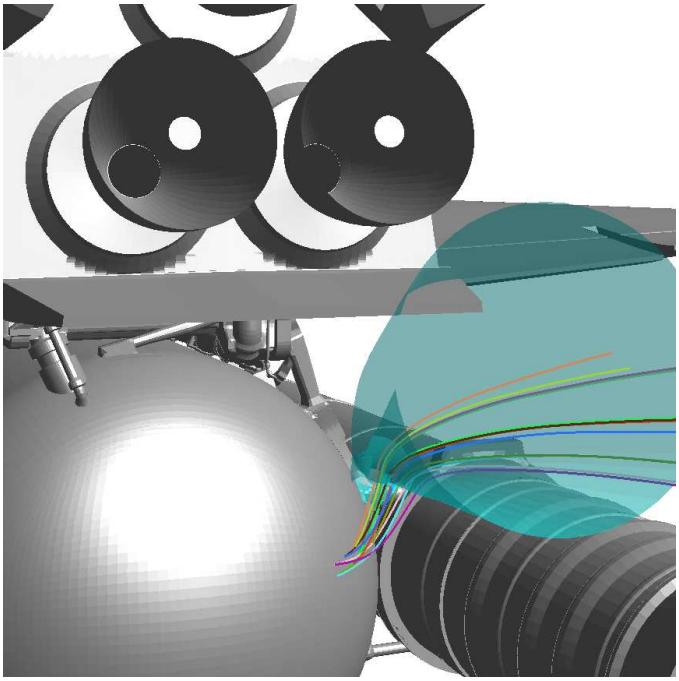

Figure 30: Trajectories of ice balls released from aft-most location.

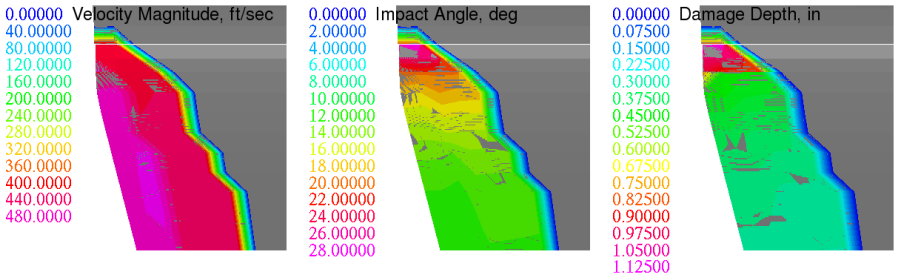

Figure 31: Impact conditions and tile-damage depth caused by the aft-most ice balls, mass=0.0022 lbm, Mach=1.4, α=-4 deg, β=-2 deg.

7 Summary

A deterministic method for analyzing the maximum allowable ice-ball size as a function of the debris-source location on the ET has been developed. It is a computationally expensive procedure relative to typical debris-transport analyses. It requires the computation of millions of debris trajectories, and then the analysis of billions of possible impacts. The method was used to compute the maximum allowable diameter for hemisphere ice-ball debris liberated from the surface of the ET for impacts on the wing leading-edge RCC, nosecap RCC, and Orbiter tiles. Detailed plots of this data illustrate that the threat posed by such ice balls is worst at the nose of the ET and generally decreases further aft. However, certain aft regions which are outboard of the aft-attach hardware have very small allowable sizes.

References

[1] "Space Shuttle Ice/Debris Inspection Criteria," NASA Document No. NSTS 08303, Revision D, NASA Johnson Space Center, June 2006.

[2] Stuart, P., "Debris Tracking Program v0.7.4 Theory," NASA Johnson Space Center, May 2006.

[3] Rogers, S. E. and Stuart, P., "Dprox: Debris Proximity and Impact Software v0.7.4," NASA Ames Research Center, May 2006.

[4] Murman, S.M., Aftosmis, M. J., and Rogers, S. E., "Characterization of Space Shuttle Ascent Debris Using CFD Methods," AIAA Paper 2005-1223, Jan. 2005.

[5] "External Tank Ice Debris Sources," slides presented at the Design Verification Review, April 5th, 2005.

[6] "RCC Expected Failure Distribution for PRA (Ice Debris)," slides presented to the SE&I TIM meeting, May 24th, 2005, Darwin Moon, DYNA RCC Damage Threshold Team.

[7] "SRB Debris Impact Analysis," Slides presented at the Design Verification Review, Math 18th, 2005, Mike Wyckoff, USA-SRB Element, SA-PRES-02836-2005-R2.

[8] P.G. Buning, R.J. Gomez, and W.I. Scallion, "CFD Approaches for Simulation of Wing-Body Stage Separation," AIAA Paper 2004-4838, AIAA 22nd Applied Aerodynamics Conference, Providence, RI, Aug. 2004.

[9] Gomez, R. J., Vicker, D., Rogers, S. E., Aftosmis, M. J., Chan, W. M., Meakin, R., and Murman, S., " STS-107 Investigation Ascent CFD Support," AIAA Paper 2004-2226, June 2004.

[10] "Mean Assessment of Ice Damage for Limited Zones/Ground Rules for Expected/Mean Ice Map," Parker, P., Leinmiller, A., Belknap, S., Murphy, L., Dunham, M., SR2948, OCCB, June 28, 2005.

[11] "Working Group Charts to Address Action Items from Jan 26-27 Debris Summit," Parker, P., Dunham, M., Rayos, E., and Leinmiller, A., Orbiter SLD, February 13, 2006.

[12] Ice Damage Software, version 1.0, dated November 1, 2005, received via email from Dr. James D. Walker, Southwest Research Institute.

A Mass and Ice-Ball Size

The following table lists the masses that were used in the debris transport of the ice balls. It also lists the liberated hemisphere diameter used in the debris transport, and the corresponding observed ice-ball diameter as would be seen on the ET before launch. The observed diameters for thin- and thick-shelled ice balls are plotted versus liberated mass in Figure 32. The symbols in the plots represent the discrete mass values that were used in the debris transport analysis of the current work.

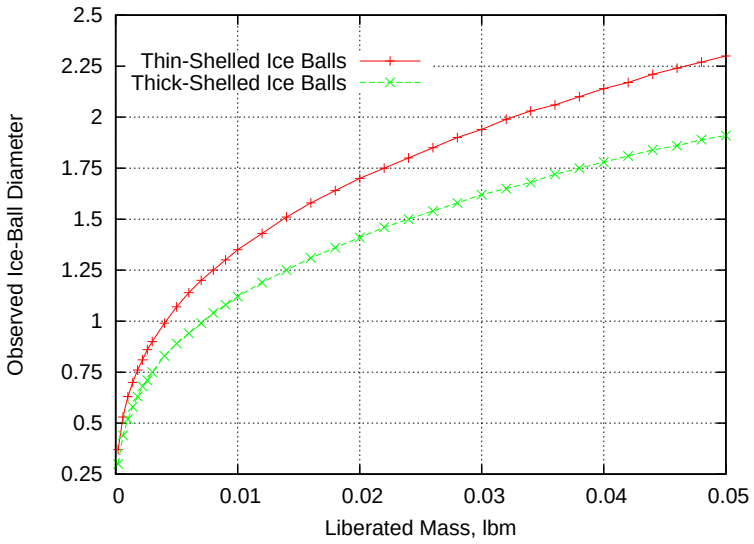

Figure 32: Relationship between liberated mass and observed diameters.

Table 1: Ice-Ball Mass and Diameter

Mass	Thin-shelled Liberated Diameter, in	Thick-shelled Liberated Diameter, in	Thin-shelled Observed Diameter, in	Thick-shelled Observed Diameter, in
0.0002	0.37	0.30	0.37	0.35
0.0006	0.53	0.44	0.53	0.50
0.0010	0.63	0.52	0.63	0.60
0.0014	0.70	0.58	0.70	0.67
0.0018	0.76	0.63	0.76	0.73
0.0022	0.81	0.68	0.81	0.78
0.0026	0.86	0.71	0.86	0.82
0.0030	0.90	0.75	0.90	0.86
0.0040	0.99	0.83	0.99	0.95
0.0050	1.07	0.89	1.07	1.02
0.0060	1.14	0.94	1.14	1.08
0.0070	1.20	0.99	1.20	1.14
0.0080	1.25	1.04	1.25	1.19
0.0090	1.30	1.08	1.30	1.24
0.0100	1.35	1.12	1.35	1.29
0.0120	1.43	1.19	1.43	1.37
0.0140	1.51	1.25	1.51	1.44
0.0160	1.58	1.31	1.58	1.50
0.0180	1.64	1.36	1.64	1.56
0.0200	1.70	1.41	1.70	1.62
0.0220	1.75	1.46	1.75	1.67
0.0240	1.80	1.50	1.80	1.72
0.0260	1.85	1.54	1.85	1.77
0.0280	1.90	1.58	1.90	1.81
0.0300	1.94	1.62	1.94	1.85
0.0320	1.99	1.65	1.99	1.89
0.0340	2.03	1.68	2.03	1.93
0.0360	2.06	1.72	2.06	1.97
0.0380	2.10	1.75	2.10	2.01
0.0400	2.14	1.78	2.14	2.04
0.0420	2.17	1.81	2.17	2.07
0.0440	2.21	1.84	2.21	2.11
0.0460	2.24	1.86	2.24	2.14
0.0480	2.27	1.89	2.27	2.17
0.0500	2.30	1.91	2.30	2.20

B CFD Flow Conditions

The following table lists the flight conditions that were used to generate the 31 different CFD cases used in the debris transport of the ice balls. The table lists the Mach number, dynamic pressure (*Qbar*) in pcf, angle of attack (α) in degrees, and side-slip angle (β) in degrees.

Table 2: CFD Flow Conditions

Mach	*Qbar*, psf	α, deg	β, deg
0.60	399.3	-3.4	0.4
0.90	640.4	-3.5	0.0
1.05	687.3	-4.0	0.0
1.10	692.5	-4.1	0.0
1.25	708.6	-4.2	0.0
1.40	718.0	-4.1	0.0
1.55	715.3	-3.7	0.0
1.80	686.9	-2.1	0.0
2.00	645.6	-1.0	0.0
2.20	583.6	0.5	0.0
2.50	452.9	2.2	0.0
2.75	353.8	2.4	0.0
3.00	268.5	2.4	0.0
3.50	137.2	2.6	0.0
1.40	814.0	-4.0	-2.0
1.40	814.0	-4.0	2.0
1.40	814.0	-6.5	0.0
1.40	814.0	-2.0	0.0
1.55	819.0	-4.0	-2.0
1.55	819.0	-4.0	2.0
1.55	819.0	-6.0	0.0
1.55	819.0	-2.0	0.0
1.80	813.0	-2.0	-2.0
1.80	813.0	-2.0	2.0
1.80	813.0	-6.0	0.0
1.80	813.0	-4.0	0.0
1.80	813.0	0.0	0.0
2.20	780.0	0.0	-2.0
2.20	780.0	0.0	2.0
2.20	780.0	-4.0	0.0
2.20	780.0	4.0	0.0

C Maximum Ice Ball Tables

The tables of the maximum allowable ice-ball diameters, in inches, are included here. Two tables are in this appendix, one for thick-shelled ice balls, the other for thin-shelled ice balls. Each table lists the maximum allowable diameter for sections of 25 inches in XT and 10 degrees in ϕ on the ET. The data in these tables is the same data that is plotted in Figures 14 and 15. For the thin-shelled ice balls, the quantity listed here is that of the inner diameter D of the ice-ball ring as illustrated in Figure 4. For thick-shelled ice balls, the quantity listed here is the outer diameter OD as illustrated in Figure 3.

Table 3: Thin-Shelled Ice-Ball Maximum Diameter, inches: -180 deg $\leq \phi \leq$ 0

XT/ϕ	-110:-100	-100:-90	-90:-80	-80:-70	-70:-60	-60:-50	-50:-40	-40:-30	-30:-20	-20:-10	-10:0
370:395	2.30	0.37	0.37	0.37	0.37	0.37	0.37	0.00	0.00	0.00	0.00
395:420	2.30	2.30	0.37	0.37	0.37	0.37	0.37	0.00	0.00	0.00	0.00
420:445	2.30	2.30	0.37	0.37	0.37	0.37	0.37	0.00	0.00	0.00	0.00
445:470	2.30	2.30	0.37	0.37	0.37	0.37	0.37	0.00	0.00	0.00	0.00
470:495	2.30	2.30	0.37	0.37	0.37	0.37	0.37	0.00	0.00	0.00	0.00
495:520	2.30	2.30	0.37	0.37	0.37	0.37	0.37	0.00	0.00	0.00	0.00
520:545	2.30	2.30	0.37	0.37	0.37	0.37	0.37	0.00	0.00	0.00	0.00
545:570	2.30	2.30	2.30	0.37	0.37	0.37	0.37	0.00	0.00	0.00	0.00
570:595	2.30	2.30	0.37	0.37	0.37	0.37	0.37	0.37	0.00	0.00	0.00
595:620	2.30	2.30	0.37	0.37	0.37	0.37	0.37	0.37	0.00	0.00	0.00
620:645	2.30	2.30	0.37	0.37	0.37	0.37	0.37	0.37	0.00	0.00	0.00
645:670	2.30	2.30	0.37	0.37	0.37	0.37	0.37	0.37	0.00	0.00	0.00
670:695	2.30	0.53	0.37	0.37	0.37	0.37	0.37	0.37	0.00	0.00	0.00
695:720	1.51	0.53	0.37	0.37	0.37	0.37	0.37	0.37	0.53	0.53	0.53
720:745	1.43	0.53	0.37	0.37	0.37	0.37	0.53	0.53	0.53	0.53	0.53
745:770	1.90	0.63	0.37	0.37	0.37	0.53	0.53	0.53	0.63	0.63	0.53
770:795	2.30	0.90	0.53	0.53	0.37	0.53	0.63	0.63	0.63	0.70	0.70
795:820	2.30	2.30	0.37	0.37	0.37	0.53	0.63	0.70	0.70	0.70	0.70
820:845	2.30	2.30	0.37	0.37	0.37	0.53	0.53	0.53	0.63	0.63	0.63
845:870	2.30	2.30	0.37	0.37	0.37	0.37	0.37	0.53	0.53	0.53	0.53
870:895	2.30	2.30	0.37	0.37	0.37	0.37	0.37	0.53	0.53	0.53	0.37
895:920	2.30	2.30	0.37	0.37	0.37	0.37	0.37	0.53	0.53	0.53	0.53
920:945	2.30	2.30	0.37	0.37	0.37	0.37	0.37	0.53	0.53	0.53	0.37
945:970	2.30	2.30	0.37	0.37	0.37	0.37	0.37	0.53	0.53	0.37	0.37
970:995	2.30	2.30	0.53	0.53	0.37	0.37	0.37	0.53	0.53	0.37	0.37
995:1020	2.30	1.64	0.53	0.53	0.53	0.53	0.53	0.53	0.37	0.37	0.53
1020:1045	2.30	0.86	0.63	0.70	0.53	0.53	0.53	0.53	0.37	0.37	0.37
1045:1070	1.58	0.81	0.53	0.90	0.70	0.70	0.53	0.53	0.37	0.37	0.53
1070:1095	2.30	0.70	0.53	0.99	0.90	0.81	0.53	0.53	0.53	0.53	0.53
1095:1120	0.53	0.53	0.53	1.07	0.90	0.90	0.63	0.53	0.53	0.53	0.53
1120:1145	0.53	0.53	0.53	1.25	0.76	1.07	0.81	0.90	0.63	0.53	0.53
1145:1170	0.53	0.53	0.53	1.35	0.53	0.99	1.35	1.07	0.86	0.53	0.53
1170:1195	0.53	0.53	0.53	1.14	0.90	1.07	1.30	1.20	0.99	0.63	0.70
1195:1220	2.30	2.30	0.81	1.75	1.07	1.14	1.30	1.35	1.07	0.70	0.86
1220:1245	2.30	2.30	2.30	2.30	1.25	1.30	1.43	1.43	1.14	0.70	0.90
1245:1270	2.30	2.30	2.30	2.30	1.35	1.43	1.58	1.51	1.20	0.90	1.25
1270:1295	2.30	2.30	2.30	2.30	1.43	1.51	1.51	1.43	1.30	1.14	1.07
1295:1320	2.30	2.30	2.30	2.30	1.51	1.51	1.51	1.43	1.43	1.30	1.07
1320:1345	2.30	2.30	2.30	2.30	1.51	1.51	1.51	1.43	1.51	1.58	1.14
1345:1370	2.30	2.30	2.30	2.10	0.99	1.58	1.58	1.51	1.51	1.85	0.90
1370:1395	2.30	2.30	2.30	1.99	1.51	1.58	1.51	1.43	1.43	1.85	0.99
1395:1420	2.30	2.30	2.30	2.17	1.51	1.64	1.51	1.43	1.43	1.85	1.30
1420:1445	2.30	2.30	2.30	2.30	1.51	1.70	1.51	1.43	1.43	1.85	1.94
1445:1470	2.30	2.30	2.30	1.90	1.58	1.70	1.43	1.35	1.43	1.80	1.80
1470:1495	2.30	2.30	2.30	1.90	1.70	1.75	1.35	1.30	1.51	1.75	1.80
1500:1525	2.30	2.30	2.30	1.80	1.70	1.80	1.30	1.25	1.51	1.94	1.85
1525:1550	2.30	2.30	2.30	1.75	1.75	1.70	1.25	1.25	1.51	1.90	2.10
1550:1575	2.30	2.30	2.30	1.75	1.64	1.70	1.25	1.25	1.51	1.90	2.10
1575:1600	2.30	2.30	2.30	2.06	1.58	1.75	1.30	1.25	1.43	1.90	2.10
1600:1625	2.30	2.30	2.30	2.03	1.64	1.70	1.30	1.25	1.43	1.85	2.06
1625:1650	2.30	2.30	2.30	2.03	1.64	1.70	1.35	1.30	1.35	1.75	2.03
1650:1675	2.30	2.30	2.30	2.30	1.58	1.75	1.35	1.30	1.35	1.70	2.03
1675:1700	2.30	2.30	2.30	2.30	1.51	1.70	1.43	1.35	1.35	1.70	1.94
1700:1725	2.30	2.30	2.30	1.90	0.81	0.86	1.58	1.35	1.43	1.75	1.85
1725:1750	2.30	2.30	2.30	2.30	0.76	0.81	1.80	1.43	1.51	1.75	1.90
1750:1775	2.30	2.30	2.30	2.30	0.81	0.70	1.14	1.58	1.58	1.75	1.90
1775:1800	2.30	2.30	2.30	2.30	0.76	0.70	1.94	1.75	1.75	1.90	1.99
1800:1825	2.30	2.30	2.30	2.30	1.07	0.81	2.30	2.10	2.03	1.75	1.85
1825:1850	2.30	2.30	2.30	2.30	0.63	0.70	2.30	2.30	2.06	1.85	1.90
1850:1875	2.30	2.30	2.30	2.30	2.30	0.81	1.51	2.21	1.85	1.58	1.51
1875:1900	2.30	2.30	2.30	2.30	0.86	0.63	0.90	1.51	1.85	1.51	2.21
1900:1925	2.30	2.30	2.30	2.30	0.63	0.70	0.90	1.14	2.06	2.30	2.30
1925:1950	2.30	2.30	2.30	0.86	0.63	0.86	0.70	1.43	2.24	1.85	2.21
1950:1975	2.30	2.30	2.30	0.53	0.53	0.76	0.70	1.94	2.30	2.30	2.30
1975:2000	2.30	2.30	2.30	0.53	0.70	0.90	0.81	1.94	2.30	2.30	2.30
2000:2025	2.30	2.30	1.43	0.37	0.37	0.37	0.81	2.06	2.30	2.30	2.30
2025:2050	2.30	2.30	2.30	0.37	0.37	2.30	0.63	2.30	2.30	2.30	2.30
2050:2075	2.30	2.30	2.30	1.75	0.81	1.30	1.07	2.30	2.30	2.30	2.30
2075:2100	2.30	2.30	2.30	2.21	0.70	1.70	1.80	2.30	1.43	1.07	2.30
2100:2125	2.30	2.30	2.30	2.30	0.81	2.30	2.30	2.10	1.43	0.90	2.30
2125:2150	2.30	1.75	2.30	2.30	2.30	2.30	1.58	1.51	1.64	2.14	2.17

Table 4: Thin-Shelled Ice-Ball Maximum Diameter, inches: $0 \leq \phi \leq 180$ deg

XT/ϕ	0:10	10:20	20:30	30:40	40:50	50:60	60:70	70:80	80:90	90:100	100:110
370:395	0.00	0.00	0.00	0.00	0.37	0.37	0.37	0.37	0.53	0.53	2.30
395:420	0.00	0.00	0.00	0.00	0.37	0.37	0.37	0.37	0.53	2.30	2.30
420:445	0.00	0.00	0.00	0.00	0.37	0.37	0.37	0.37	0.37	2.30	2.30
445:470	0.00	0.00	0.00	0.00	0.37	0.37	0.37	0.37	0.37	2.30	2.30
470:495	0.00	0.00	0.00	0.00	0.37	0.37	0.37	0.37	0.37	2.30	2.30
495:520	0.00	0.00	0.00	0.00	0.37	0.37	0.37	0.37	0.37	2.30	2.30
520:545	0.00	0.00	0.00	0.00	0.37	0.37	0.37	0.37	0.37	2.30	2.30
545:570	0.00	0.00	0.00	0.00	0.37	0.37	0.37	0.37	2.30	2.30	2.30
570:595	0.00	0.00	0.00	0.37	0.37	0.37	0.37	0.37	0.37	2.30	2.30
595:620	0.00	0.00	0.00	0.37	0.37	0.37	0.37	0.37	0.37	2.30	2.30
620:645	0.00	0.00	0.00	0.37	0.37	0.37	0.37	0.37	0.37	2.30	2.30
645:670	0.00	0.00	0.00	0.37	0.37	0.37	0.37	0.37	0.37	2.30	2.30
670:695	0.00	0.00	0.00	0.37	0.53	0.37	0.37	0.37	0.37	0.53	2.30
695:720	0.53	0.53	0.53	0.53	0.53	0.37	0.37	0.37	0.37	0.53	1.35
720:745	0.53	0.53	0.53	0.53	0.53	0.53	0.37	0.37	0.37	0.53	1.30
745:770	0.53	0.53	0.37	0.63	0.63	0.53	0.37	0.53	0.53	0.63	1.80
770:795	0.53	0.53	0.37	0.63	0.63	0.53	0.37	0.53	0.53	0.90	2.27
795:820	0.70	0.63	0.37	0.37	0.63	0.53	0.37	0.37	0.37	2.30	2.30
820:845	0.53	0.37	0.53	0.53	0.53	0.53	0.37	0.37	0.37	2.30	2.30
845:870	0.53	0.63	0.37	0.63	0.53	0.37	0.37	0.37	0.37	2.30	2.30
870:895	0.53	0.37	0.37	0.63	0.53	0.37	0.37	0.37	0.37	2.30	2.30
895:920	0.53	0.37	0.37	0.53	0.37	0.37	0.37	0.37	0.37	2.30	2.30
920:945	0.53	0.37	0.37	0.53	0.53	0.37	0.37	0.37	0.37	2.30	2.30
945:970	0.53	0.53	0.37	0.37	0.53	0.37	0.37	0.37	0.53	2.30	2.30
970:995	0.37	0.37	0.53	0.53	0.53	0.37	0.37	0.53	0.53	2.30	2.30
995:1020	0.53	0.53	2.30	0.53	0.63	0.70	0.53	0.70	0.63	0.81	2.30
1045:1070	0.53	0.53	0.37	0.53	0.81	0.76	0.81	0.86	0.63	0.90	1.99
1070:1095	0.90	0.63	0.53	0.53	0.81	0.90	0.90	0.99	0.63	0.99	1.43
1095:1120	1.14	1.43	0.53	0.99	0.90	1.07	1.43	0.99	0.53	0.90	0.63
1120:1145	1.14	1.20	0.53	0.53	1.51	1.35	0.90	1.25	0.53	0.53	0.53
1145:1170	0.70	0.53	0.53	0.53	1.64	1.35	1.07	1.20	0.63	0.53	0.53
1170:1195	0.81	0.76	0.70	0.86	1.58	1.64	1.07	0.81	0.53	0.53	0.53
1195:1220	0.76	0.76	0.63	1.14	1.64	1.64	0.86	1.35	1.25	0.53	0.53
1220:1245	0.81	0.81	0.63	0.90	1.75	1.51	0.90	1.35	1.25	1.90	2.30
1245:1270	0.86	0.86	0.63	0.90	1.75	1.58	1.43	2.30	1.70	1.85	2.30
1270:1295	0.86	0.90	0.70	0.81	1.75	1.43	1.14	2.30	2.24	2.30	2.30
1295:1320	0.86	0.81	0.81	1.14	1.51	1.58	1.58	2.30	2.30	2.30	2.30
1320:1345	0.86	0.81	0.86	1.64	1.51	1.51	1.14	2.30	2.30	2.30	2.30
1345:1370	0.86	0.81	0.90	1.58	1.43	1.51	1.35	2.30	2.30	2.30	2.30
1370:1395	0.86	0.86	1.51	0.90	1.35	1.43	1.35	2.03	2.30	2.30	2.30
1395:1420	0.90	1.80	1.35	1.90	1.30	1.43	1.35	2.17	2.30	2.30	2.30
1420:1445	1.64	1.80	1.25	1.14	1.25	1.58	1.58	2.17	2.30	2.30	2.30
1445:1470	1.64	1.58	1.20	0.99	1.30	1.58	1.51	1.80	2.30	2.30	2.30
1470:1495	1.58	1.43	1.43	1.70	1.25	1.70	1.70	1.75	2.30	2.30	2.30
1500:1525	1.58	1.43	1.07	0.76	1.20	1.64	1.64	1.75	2.30	2.30	2.30
1525:1550	1.58	1.30	0.99	1.35	1.25	1.85	1.75	1.85	2.30	2.30	2.30
1550:1575	1.99	1.58	0.99	1.64	1.35	1.80	1.75	1.94	2.30	2.30	2.30
1575:1600	1.80	1.58	1.25	0.99	1.35	1.75	1.85	2.17	2.30	2.30	2.30
1600:1625	1.64	1.35	1.30	1.51	0.90	1.80	1.85	2.10	2.30	2.30	2.30
1625:1650	1.64	1.25	1.07	1.43	0.90	1.51	2.03	2.14	2.30	2.30	2.30
1650:1675	1.43	1.20	1.07	1.80	0.99	0.76	1.94	2.24	2.30	2.30	2.30
1675:1700	2.03	1.35	1.14	1.80	1.58	0.76	1.85	2.30	2.30	2.30	2.30
1700:1725	1.75	1.35	1.14	1.90	0.90	0.90	0.90	2.30	2.30	2.30	2.30
1725:1750	1.70	1.51	1.14	1.75	0.76	0.70	0.90	2.30	2.30	2.30	2.30
1750:1775	2.21	1.43	1.07	1.35	1.35	0.70	1.07	2.30	2.30	2.30	2.30
1775:1800	2.30	1.64	1.07	1.30	1.51	0.63	0.90	2.30	2.30	2.30	2.30
1800:1825	2.24	1.30	0.76	0.90	1.58	0.81	0.76	2.30	2.30	2.30	2.30
1825:1850	2.03	1.43	0.76	1.70	1.51	0.70	0.76	2.30	2.30	2.30	2.30
1850:1875	1.94	1.58	1.35	1.35	1.35	0.81	0.53	1.30	2.30	2.30	2.30
1875:1900	2.30	1.80	1.75	1.43	1.51	0.81	0.63	1.64	2.30	2.30	2.30
1900:1925	2.30	2.30	1.64	1.75	1.25	0.90	0.53	2.30	2.30	2.30	2.30
1925:1950	2.30	2.14	2.03	0.81	1.25	0.76	0.63	1.43	2.30	2.30	2.30
1950:1975	2.30	2.30	2.30	2.30	1.14	0.70	0.37	0.70	2.30	2.30	2.30
1975:2000	2.30	2.30	2.30	1.07	1.07	1.43	0.63	0.53	2.30	2.30	2.30
2000:2025	2.30	2.30	2.30	0.90	0.90	0.70	0.53	0.53	1.07	2.30	2.30
2025:2050	2.30	2.30	1.58	1.35	0.86	2.30	0.37	0.53	2.30	2.30	2.30
2050:2075	2.30	2.30	2.30	2.30	2.30	2.30	0.81	2.30	2.30	2.30	2.30
2075:2100	2.30	2.30	2.30	2.30	2.30	1.58	0.63	2.30	2.30	2.30	2.30
2100:2125	1.30	2.30	2.30	2.30	2.30	1.58	0.63	0.63	1.58	2.30	2.30
2125:2150	2.30	1.30	2.30	2.30	2.30	1.64	0.86	0.76	0.76	1.14	2.30

Table 5: Thick-Shelled Ice-Ball Maximum Diameter, inches: -180 deg $\leq \phi \leq$ 0

XT/ϕ	-110:-100	-100:-90	-90:-80	-80:-70	-70:-60	-60:-50	-50:-40	-40:-30	-30:-20	-20:-10	-10:0
370:395	2.25	0.36	0.36	0.36	0.36	0.36	0.36	0.00	0.00	0.00	0.00
395:420	2.25	1.90	0.36	0.36	0.36	0.36	0.36	0.00	0.00	0.00	0.00
420:445	2.25	2.25	0.36	0.36	0.36	0.36	0.36	0.00	0.00	0.00	0.00
445:470	2.25	2.25	0.36	0.36	0.36	0.36	0.36	0.00	0.00	0.00	0.00
470:495	2.25	2.25	0.36	0.36	0.36	0.36	0.36	0.00	0.00	0.00	0.00
495:520	2.25	2.25	0.36	0.36	0.36	0.36	0.36	0.00	0.00	0.00	0.00
520:545	2.25	2.25	0.36	0.36	0.36	0.36	0.36	0.00	0.00	0.00	0.00
545:570	2.25	2.25	2.25	0.36	0.36	0.36	0.36	0.00	0.00	0.00	0.00
570:595	2.25	2.25	0.36	0.36	0.36	0.36	0.36	0.36	0.00	0.00	0.00
595:620	2.25	2.25	0.52	0.36	0.36	0.36	0.36	0.36	0.00	0.00	0.00
620:645	2.25	2.25	0.52	0.52	0.52	0.36	0.36	0.52	0.00	0.00	0.00
645:670	2.25	2.25	0.52	0.52	0.52	0.52	0.52	0.52	0.00	0.00	0.00
670:695	2.25	0.52	0.52	0.52	0.52	0.52	0.52	0.52	0.00	0.00	0.00
695:720	1.47	0.52	0.52	0.52	0.52	0.52	0.52	0.52	0.52	0.52	0.52
720:745	1.47	0.52	0.52	0.52	0.52	0.52	0.52	0.52	0.52	0.52	0.61
745:770	1.81	0.52	0.52	0.52	0.52	0.52	0.52	0.52	0.52	0.61	0.61
770:795	2.25	0.61	0.52	0.52	0.52	0.61	0.61	0.61	0.61	0.68	0.68
795:820	2.25	2.25	0.52	0.52	0.52	0.68	0.74	0.74	0.68	0.68	0.68
820:845	2.25	2.25	0.52	0.36	0.52	0.52	0.52	0.61	0.52	0.61	0.61
845:870	2.25	2.25	0.52	0.36	0.36	0.52	0.52	0.52	0.52	0.52	0.61
870:895	2.25	2.25	0.52	0.36	0.36	0.52	0.52	0.61	0.61	0.61	0.61
895:920	2.25	2.25	0.52	0.36	0.36	0.36	0.52	0.61	0.61	0.61	0.61
920:945	2.25	2.25	0.52	0.52	0.36	0.36	0.52	0.52	0.61	0.52	0.61
945:970	2.25	2.25	0.52	0.52	0.52	0.36	0.52	0.61	0.52	0.52	0.61
970:995	2.25	2.25	0.52	0.52	0.52	0.61	0.61	0.61	0.52	0.52	0.61
995:1020	2.25	1.76	0.61	0.52	0.52	0.52	0.61	0.61	0.52	0.52	0.61
1020:1045	2.25	0.97	0.68	0.68	0.61	0.61	0.52	0.52	0.52	0.52	0.52
1045:1070	1.11	0.97	0.61	1.05	0.80	0.74	0.61	0.52	0.52	0.52	0.52
1070:1095	2.25	0.74	0.61	1.17	1.05	0.88	0.61	0.52	0.52	0.52	0.52
1095:1120	0.61	0.61	0.61	1.17	0.88	0.97	0.61	0.52	0.52	0.52	0.52
1120:1145	0.61	0.61	0.61	1.22	0.80	1.22	0.97	0.88	0.74	0.61	0.61
1145:1170	0.61	0.61	0.61	1.54	0.61	1.17	1.60	1.22	0.97	0.61	0.61
1170:1195	0.61	0.61	0.61	1.27	1.05	1.22	1.54	1.32	1.17	0.68	0.80
1195:1220	2.25	2.25	2.06	2.25	1.32	1.32	1.47	1.47	1.22	0.80	0.97
1220:1245	2.25	2.25	2.25	2.25	1.40	1.40	1.47	1.40	1.22	0.84	1.05
1245:1270	2.25	2.25	2.25	2.25	1.40	1.32	1.40	1.32	1.32	0.97	1.40
1270:1295	2.25	2.25	2.25	2.25	1.47	1.40	1.32	1.32	1.32	1.27	1.22
1295:1320	2.25	2.25	2.25	2.25	1.54	1.40	1.32	1.27	1.32	1.40	1.27
1320:1345	2.25	2.25	2.25	2.25	1.40	1.47	1.40	1.27	1.32	1.71	1.54
1345:1370	2.25	2.25	2.25	2.25	1.47	1.60	1.40	1.32	1.32	1.71	1.11
1370:1395	2.25	2.25	2.25	2.22	1.47	1.66	1.40	1.27	1.27	1.71	1.17
1395:1420	2.25	2.25	2.25	2.25	1.54	1.60	1.40	1.27	1.32	1.71	1.94
1420:1445	2.25	2.25	2.25	2.25	1.54	1.60	1.32	1.32	1.32	1.66	2.02
1445:1470	2.25	2.25	2.25	1.76	1.47	1.60	1.32	1.27	1.32	1.60	2.02
1470:1495	2.25	2.25	2.25	1.76	1.60	1.66	1.32	1.22	1.32	1.76	2.06
1500:1525	2.25	2.25	2.25	1.71	1.66	1.66	1.22	1.17	1.32	1.76	2.09
1525:1550	2.25	2.25	2.25	1.66	1.60	1.47	1.22	1.11	1.32	1.76	2.09
1550:1575	2.25	2.25	2.25	1.66	1.40	1.47	1.22	1.11	1.32	1.76	2.13
1575:1600	2.25	2.25	2.25	1.98	1.32	1.54	1.17	1.11	1.32	1.76	2.09
1600:1625	2.25	2.25	2.25	1.86	1.40	1.60	1.17	1.11	1.27	1.71	2.06
1625:1650	2.25	2.25	2.25	2.25	1.40	1.54	1.22	1.17	1.27	1.60	2.02
1650:1675	2.25	2.25	2.25	2.25	1.32	1.54	1.27	1.17	1.27	1.54	2.02
1675:1700	2.25	2.25	2.25	2.25	1.32	1.47	1.32	1.22	1.27	1.60	2.02
1700:1725	2.25	2.25	2.25	2.25	1.17	1.40	1.47	1.27	1.32	1.60	1.94
1725:1750	2.25	2.25	2.25	2.25	1.05	1.54	1.86	1.32	1.32	1.66	1.94
1750:1775	2.25	2.25	2.25	2.25	1.05	1.05	1.40	1.47	1.54	1.76	1.90
1775:1800	2.25	2.25	2.25	2.25	2.25	1.11	2.02	1.66	1.71	1.86	1.94
1800:1825	2.25	2.25	2.25	2.25	2.25	2.25	2.25	2.06	1.94	1.98	2.02
1825:1850	2.25	2.25	2.25	2.25	2.25	2.25	2.25	2.25	2.25	2.06	1.86
1850:1875	2.25	2.25	2.25	2.25	2.25	0.97	2.25	2.25	2.06	2.09	2.06
1875:1900	2.25	2.25	2.25	2.25	1.76	1.22	1.47	1.86	1.94	2.13	2.06
1900:1925	2.25	2.25	2.25	2.25	0.88	1.32	1.47	1.54	2.02	2.25	2.25
1925:1950	2.25	2.25	2.25	0.97	0.97	1.27	1.22	1.47	2.25	2.25	2.25
1950:1975	2.25	2.25	2.25	0.74	0.88	0.68	1.27	1.90	2.25	2.25	2.25
1975:2000	2.25	2.25	2.25	0.84	0.88	1.22	1.54	2.25	2.25	2.25	2.25
2000:2025	2.25	2.25	1.66	0.61	0.61	0.68	1.40	1.90	2.25	2.25	2.25
2025:2050	2.25	2.25	2.25	0.61	0.68	2.25	0.84	2.25	2.25	2.25	2.06
2050:2075	2.25	2.25	2.25	1.22	0.97	2.09	2.06	2.25	2.25	2.25	2.25
2075:2100	2.25	2.25	2.25	1.47	0.97	2.25	2.25	2.25	1.94	2.16	2.25
2100:2125	2.25	2.25	2.25	2.25	1.22	2.25	2.25	2.06	1.90	1.98	2.25
2125:2150	2.25	2.25	2.25	2.25	2.25	2.25	2.25	1.81	1.90	2.13	2.25

Table 6: Thick-Shelled Ice-Ball Maximum Diameter, inches: $0 \leq \phi \leq 180$ deg

XT/ϕ	0:10	10:20	20:30	30:40	40:50	50:60	60:70	70:80	80:90	90:100	100:110
370:395	0.00	0.00	0.00	0.00	0.36	0.36	0.36	0.52	0.52	0.52	2.25
395:420	0.00	0.00	0.00	0.00	0.36	0.36	0.36	0.52	0.52	1.76	2.25
420:445	0.00	0.00	0.00	0.00	0.36	0.36	0.36	0.36	0.52	2.25	2.25
445:470	0.00	0.00	0.00	0.00	0.36	0.36	0.36	0.36	0.36	2.25	2.25
470:495	0.00	0.00	0.00	0.00	0.36	0.36	0.36	0.36	0.36	2.25	2.25
495:520	0.00	0.00	0.00	0.00	0.36	0.36	0.36	0.36	0.36	2.25	2.25
520:545	0.00	0.00	0.00	0.00	0.36	0.36	0.36	0.36	0.36	2.25	2.25
545:570	0.00	0.00	0.00	0.00	0.36	0.36	0.36	0.36	2.25	2.25	2.25
570:595	0.00	0.00	0.00	0.36	0.36	0.36	0.36	0.36	0.52	2.25	2.25
595:620	0.00	0.00	0.00	0.36	0.36	0.36	0.36	0.52	0.52	2.25	2.25
620:645	0.00	0.00	0.00	0.52	0.52	0.36	0.52	0.52	0.52	2.25	2.25
645:670	0.00	0.00	0.00	0.52	0.52	0.52	0.52	0.52	0.52	2.25	2.25
670:695	0.00	0.00	0.00	0.52	0.52	0.52	0.52	0.52	0.52	0.52	2.25
695:720	0.52	0.61	0.61	0.52	0.52	0.52	0.52	0.52	0.52	0.52	1.32
720:745	0.52	0.61	0.68	0.61	0.61	0.52	0.52	0.52	0.52	0.52	1.27
745:770	0.52	0.61	0.68	0.61	0.61	0.61	0.52	0.52	0.52	0.52	1.81
770:795	0.61	0.61	0.68	0.68	0.61	0.61	0.52	0.52	0.52	0.61	2.25
795:820	0.61	0.61	0.61	0.61	0.74	0.74	0.52	0.52	0.52	2.25	2.25
820:845	0.61	0.61	0.61	0.61	0.61	0.52	0.52	0.36	0.36	2.25	2.25
845:870	0.61	0.68	0.61	0.61	0.61	0.52	0.36	0.36	0.52	2.25	2.25
870:895	0.61	0.61	0.68	0.68	0.52	0.52	0.36	0.36	0.52	2.25	2.25
895:920	0.61	0.61	0.52	0.61	0.52	0.52	0.36	0.36	0.52	2.25	2.25
920:945	0.61	0.61	0.52	0.61	0.52	0.36	0.36	0.52	0.52	2.25	2.25
945:970	0.61	0.61	0.52	0.52	0.61	0.52	0.36	0.52	0.52	2.25	2.25
970:995	0.52	0.61	0.52	0.52	0.61	0.61	0.52	0.52	0.52	2.25	2.25
995:1020	0.52	0.52	2.25	0.52	0.61	0.61	0.61	0.52	0.52	1.54	2.25
1020:1045	0.68	0.61	2.25	0.61	0.68	0.74	0.61	0.68	0.68	0.88	2.25
1045:1070	0.88	0.61	0.52	0.61	0.84	0.80	0.84	1.05	0.61	1.11	1.54
1070:1095	1.11	1.54	0.52	0.68	0.80	0.97	1.11	1.11	0.61	1.05	1.47
1095:1120	1.22	2.02	0.52	1.27	0.84	1.11	1.40	1.17	0.61	0.68	0.97
1120:1145	1.27	1.27	0.52	0.68	1.54	1.66	1.05	1.32	0.61	0.61	0.61
1145:1170	0.84	0.61	0.61	0.52	2.02	1.66	1.17	1.22	0.61	0.61	0.61
1170:1195	0.88	0.84	0.74	0.97	1.86	1.76	1.22	0.88	0.61	0.61	0.61
1195:1220	0.84	0.84	0.68	1.40	1.76	1.76	1.47	1.11	1.32	1.47	0.61
1220:1245	0.88	0.88	0.74	0.97	1.54	1.47	1.47	1.76	1.32	1.86	2.25
1245:1270	0.88	0.88	0.74	1.11	1.47	1.60	1.47	2.25	1.81	2.25	2.25
1270:1295	0.88	0.97	0.74	0.84	1.60	1.47	1.40	2.25	2.25	2.25	2.25
1295:1320	0.88	0.88	0.84	0.97	1.40	1.54	1.54	2.25	2.25	2.25	2.25
1320:1345	0.88	0.88	0.88	1.47	1.32	1.60	1.32	2.25	2.25	2.25	2.25
1345:1370	0.88	0.88	0.88	1.40	1.40	1.60	1.66	2.25	2.25	2.25	2.25
1370:1395	0.88	0.88	2.16	1.22	1.32	1.60	1.47	2.25	2.25	2.25	2.25
1395:1420	1.05	1.86	1.98	1.81	1.22	1.60	1.40	2.25	2.25	2.25	2.25
1420:1445	2.02	1.86	1.71	1.47	1.22	1.54	1.47	2.25	2.25	2.25	2.25
1445:1470	1.98	1.90	1.71	1.27	1.22	1.54	1.47	1.90	2.25	2.25	2.25
1470:1495	2.02	1.86	1.81	2.16	1.22	1.66	1.47	1.94	2.25	2.25	2.25
1500:1525	1.94	1.76	1.71	1.17	1.17	1.71	1.47	2.02	2.25	2.25	2.25
1525:1550	2.02	1.71	1.66	1.86	1.22	1.71	1.54	1.86	2.25	2.25	2.25
1550:1575	2.06	2.02	1.76	1.54	1.22	1.60	1.66	1.98	2.25	2.25	2.25
1575:1600	1.90	1.98	1.86	1.22	1.22	1.54	2.13	2.25	2.25	2.25	2.25
1600:1625	1.90	2.02	1.98	1.40	1.27	1.60	2.09	2.25	2.25	2.25	2.25
1625:1650	2.13	2.16	1.47	1.32	1.22	1.60	2.02	2.25	2.25	2.25	2.25
1650:1675	2.16	2.22	1.40	1.54	1.40	1.60	1.98	2.25	2.25	2.25	2.25
1675:1700	2.22	2.25	1.47	2.02	1.54	1.60	1.98	2.25	2.25	2.25	2.25
1700:1725	2.02	2.13	1.76	2.02	1.32	1.54	2.02	2.25	2.25	2.25	2.25
1725:1750	2.06	2.13	1.54	1.71	1.17	1.05	1.98	2.25	2.25	2.25	2.25
1750:1775	2.13	2.16	1.40	2.22	1.47	0.97	1.60	2.25	2.25	2.25	2.25
1775:1800	2.25	1.76	1.47	1.86	1.47	0.97	1.60	2.25	2.25	2.25	2.25
1800:1825	2.16	2.25	1.32	1.11	1.60	1.32	1.27	2.25	2.25	2.25	2.25
1825:1850	2.19	2.19	1.27	1.66	1.54	1.11	1.11	2.25	2.25	2.25	2.25
1850:1875	2.25	2.02	1.86	1.32	1.17	1.22	0.88	2.25	2.25	2.25	2.25
1875:1900	2.25	2.02	1.54	1.71	1.98	1.17	0.84	1.98	2.25	2.25	2.25
1900:1925	2.25	2.25	1.47	1.98	1.98	1.11	1.05	2.25	2.25	2.25	2.25
1925:1950	2.25	2.25	1.86	1.71	1.32	0.80	0.84	1.76	2.25	2.25	2.25
1950:1975	2.25	2.25	2.25	2.25	1.22	1.11	0.74	1.54	2.25	2.25	2.25
1975:2000	2.25	2.25	2.25	2.25	1.40	1.54	0.84	0.97	2.25	2.25	2.25
2000:2025	2.25	2.25	2.25	1.11	1.32	1.40	0.84	0.68	1.32	2.25	2.25
2025:2050	2.25	2.25	2.25	1.81	1.54	2.25	0.97	0.97	2.25	2.25	2.25
2050:2075	2.25	2.25	2.25	2.25	2.25	2.25	1.76	2.25	2.25	2.25	2.25
2075:2100	2.25	2.25	2.25	2.25	2.25	2.25	0.88	2.25	2.25	2.25	2.25
2100:2125	2.25	2.25	2.25	2.25	2.25	2.25	0.97	0.97	1.27	2.25	2.25
2125:2150	2.25	2.25	2.25	2.25	2.25	2.25	2.25	1.05	1.05	2.25	2.25